

# **Capstone Project: Aero Rider**

## **Practice of Mechanical Engineering 2024 Spring**

Group 4

B10502021 周知穎

B10502039 張伯宇

B10502063 張曜鵬

B10502064 王泰傑

B10502024 蔡家凱

## Abstract

The Aero Rider project, as a capstone for practical mechanical engineering, aimed to design and develop an autonomous wind-powered vehicle using sail control for optimal performance. This project emphasized system integration, innovative design, and the application of theoretical knowledge within stringent size, weight, and budget constraints. The vehicle employed a Proportional-Derivative (PD) control system for sail adjustment, enabling precise path control through yaw manipulation. Encoder feedback and Inertial Measurement Unit (IMU) sensors maintained stability and direction, with servo motors dynamically adjusting the sail to varying wind conditions.

The design process involved detailed analysis and optimization of the sail deployment mechanism, chassis, and electromechanical systems. Finite Element Analysis (FEA) was conducted to enhance the chassis structure for both strength and weight efficiency. Dynamic response testing of the sail control system verified its performance, ensuring that the vehicle could autonomously deploy its sails and travel the maximum possible distance within a set timeframe.

Our design adhered to strict specifications: the vehicle, in its initial state, measured no more than 30 cm in length, 21 cm in width, and 40 cm in height, and weighed under 2 kg. The vehicle used universal wheels and maintained contact with the track solely through these wheels. These constraints necessitated innovative solutions within limited space and weight, ensuring stability under varying conditions. The entire electromechanical system was assembled by our team within a budget of NTD 3000, emphasizing efficient cost management.

The core concept of Aero Rider involved harnessing wind power as the driving force and controlling the sail's angle of incidence to adjust the vehicle's path. The route was segmented into five sections, with a microcontroller (MCU) and encoder feedback used to determine the vehicle's position and sail angle. PD control adjusted the sail size based on real-time feedback, avoiding inconsistencies from open-loop control methods. Flow field analysis was also conducted to optimize sail height and path, enhancing performance and stability.

Despite some challenges, the project successfully integrated mechanical and electronic control systems, demonstrating effective system integration, stability, and high performance. Aero Rider showcased our team's capability in innovative design and practical engineering application, providing a solid foundation for future improvements and stronger performance in real-world applications.

# Table of Contents

1.	Introduction.....	8
2.	Design Requirement.....	11
2.1	Navigation Strategy .....	11
2.2	Working Principle for the Chassis and Brake .....	11
2.2.1	Chassis .....	11
2.2.2	Brake.....	11
2.3	Working Principle for Control and Sail Design .....	11
2.3.1	Working principle .....	11
2.3.2	PD Control .....	13
2.3.3	Encoder Readings .....	15
2.3.4	Parameters.....	15
2.4	Working Principle for Control and Sail Design .....	15
3.	Design Concepts and Layout .....	16
3.1	System Overview .....	16
3.2	Sail Deployment.....	16
3.2.1	Lifting Mechanism.....	16
3.2.2	Sail Design.....	17
3.2.3	Sail Dimension Determination.....	18
3.2.4	Energy Transfer.....	19
3.3	Chassis Design .....	21
3.4	Design and Analysis of the Braking System.....	22
3.4.1	Braking Design Logic .....	22
3.4.2	Calculation of Braking Force.....	22
3.4.3	Working Principle of Braking Friction .....	23
3.4.4	Vehicle Dynamics Analysis.....	23
3.5	Electromechanical System .....	24
3.5.1	Power .....	24
3.5.2	Inputs.....	25
3.5.3	Outputs.....	26
3.6	Vehicle System.....	26
4.	Analysis and Verification .....	27
4.1	Rolling Friction of the Universal Wheel.....	27
4.2	Sail Analysis.....	30
4.2.1	Theoretical Analysis.....	30
4.2.2	Design Verification .....	31
4.3	Brake Analysis .....	32

4.4	Chassis Analysis.....	33
4.4.1	Static Analysis.....	33
4.5	Dynamic response of the mechatronics system .....	35
4.6	Dynamic response of the Vehicle.....	37
5.	Working Norms and Consensus .....	44
5.1	Team Contract.....	44
5.2	Gannt Chart of our Work Schedule and Some Reflection .....	45
5.3	Work Distribution .....	46
5.4	Peer Review .....	46
5.4.1	Evaluation Criteria .....	46
5.4.2	Evaluation Results .....	47
6.	Personal Reflection and Suggestions.....	48
7.	References.....	55
8.	Appendix.....	56
8.1	Bill of Materials (BOM) .....	56
8.2	Exploded View.....	58
8.2.1	Exploded View of the Whole Assembly .....	58
8.2.2	Exploded View of the Whole Chassis.....	58
8.2.3	Exploded View of the Lifting Mechanism.....	59
8.2.4	Exploded View of the Sail .....	59
8.2.5	Exploded View of the Encoder .....	60
8.3	Engineering Drawings of Crucial Components .....	60
8.3.1	Chassis .....	60
8.3.2	Brake.....	62
8.3.3	Lift.....	64
8.3.4	Sail .....	66
8.4	Meeting Minutes .....	69
8.5	Code for Testing.....	73

## List of Figures

Figure 1. The ideal route for the final test .....	11
Figure 2. The free body diagram of the vehicle .....	12
Figure 3. Simplified drawing of sail design .....	12
Figure 4. Global variables of the PID controls.....	13
Figure 5. Functions for PID controller. ....	14
Figure 6 The code for PD control .....	14
Figure 7. Rack and Pinion Design .....	16
Figure 8. Lifting Mechanism's CAD .....	16
Figure 9. Operation principle of lifting mechanism .....	17
Figure 10. V-shaped Configuration .....	17
Figure 11. Operation principle of sail mechanism when fully expanded .....	18
Figure 12. Operation principle of sail mechanism when half-expanded.....	18
Figure 13. Indication of Force Exerting on Sail .....	20
Figure 14. Vehicle Dynamics.....	20
Figure 15. CAD Model of out Chassis Design.....	21
Figure 16. The braking system (Isotropic view).....	22
Figure 17. The braking system (Front view) .....	22
Figure 18. Mechatronics Block Diagram .....	24
Figure 19. ADIO-DC36V5A voltage converter.....	24
Figure 20. Design of the encoder.....	25
Figure 21. Experiment Setup (Isometric view) .....	28
Figure 22. The forces with our experiment device (the size is not to scale) .....	28
Figure 23. Experiment Setup (top view) .....	29
Figure 24. The measuring picture of Tracker .....	29
Figure 25. Friction Coefficient vs Velocity.....	30
Figure 26. Low wind speed area (red point).....	31
Figure 27. Friction Coefficient vs Velocity .....	32
Figure 28. Stress analysis of the chassis without design. ....	34
Figure 29. Stress analysis of the chassis after design. ....	34
Figure 30. Displacement of the chassis without design.....	34
Figure 31. Displacement of the chassis after design. ....	34
Figure 32. Tracking the position of the sail tip using “Tracker” .....	35
Figure 33. The expanding response time of the sail servo motor.....	36
Figure 34. Closing response time of the sail servo motor .....	36
Figure 35. Kp=10, Kd=0.2, Set point=90 .....	38
Figure 36. Kp=10, Kd=0.4, Set point=90 .....	39

Figure 37. Kp=15, Kd=0.4, Set point=90 .....	39
Figure 38. Kp=10, Kd=0.2, Set point=60 .....	40
Figure 39. Kp=15, Kd=0.4, Set point=60 .....	41
Figure 40. Kp=10, Kd=0.2, Set point=30 .....	41
Figure 41. Kp=10, Kd=0.4, Set point=30 .....	42
Figure 42. Kp=15, Kd=0.4, Set point=30 .....	42

## **List of Tables**

Table 1. Measurement Data of the experiment.....	30
Table 2. Measurement Data of the experiment.....	32
Table 3. Rise time at different conditions .....	43
Table 4. Percent overshoot at different conditions .....	43

## 1. Introduction

The primary aim of our project, "Aero Rider," is to utilize wind power as the main driving force to achieve autonomous movement of the vehicle by controlling the sail system. The main goal of this design is to train us in practical mechanical engineering skills, enhancing our abilities in system integration, teamwork, theoretical application, and innovative thinking. Through this design and production process, we need to address and solve various technical and design challenges, thereby improving our practical engineering execution capabilities and validating our theoretical knowledge in practice.

Our design must adhere to strict specifications and constraints. The vehicle, in its initial state, must not exceed dimensions of 30cm (length)  $\times$  21cm (width)  $\times$  40cm (height), and its total weight must not exceed 2kg. The vehicle must use the designated wheel type (universal wheels), and throughout the entire competition, it can only make contact with the track through its wheels. These constraints require us to innovate within limited space and weight, ensuring the vehicle operates stably under different conditions. Additionally, the entire electromechanical system must be assembled by our team, and the total material cost must not exceed NTD 3000, emphasizing efficient cost control and resource utilization. We need to find optimal solutions within these constraints, leveraging creativity and technical skills to their fullest extent.

The primary goal of testing is to ensure that the vehicle can autonomously deploy its sails and achieve the longest possible distance within 3 minutes. We will conduct two tests in each of two different runways, using the median distance as the final result. These tests aim to verify the stability and performance of the design and provide a basis for further optimization. Through these tests, we aim to understand the actual performance of the design, identify areas for improvement, and make targeted adjustments to ensure the final design performs optimally in real-world applications.

The core concept of Aero Rider is to harness wind power as the driving force and control the sail's angle of incidence to adjust the vehicle's path. Specifically, we segment the target route into five sections, using a microcontroller (MCU) and feedback signals from an encoder wheel to determine the vehicle's position and sail angle. Based on the error between the target sail's opening angle at different distances and the current opening angle, we use PD control to adjust the sail size with different opening angles for precise path control. This method avoids the inconsistencies that may arise from time-based open-loop control due to different gliding times. We also conduct flow field analysis to design the optimal sail height and path, further enhancing the vehicle's performance and stability. This precise control not only improves movement efficiency but also ensures stable driving under different wind speeds and environments.

Our aero Rider's design features several innovative aspects, including the PD control of the opening angle of the sails and the flow field analysis to optimize the sail height and the path as mentioned in the previous paragraph. Additionally, within the constraints of our budget and resources, we successfully integrated mechanical and electronic control systems through meticulous design and iterative testing, ensuring the vehicle's stability and high performance. Our design not only demonstrates technical innovation but also reflects our team's ability to apply multidisciplinary knowledge in practical engineering projects.

The design process underwent multiple iterations and optimizations to reach the current outcome. In the initial design phase, we focused on achieving straight-line movement, basic structure, and stability. As the design progressed, we introduced control mechanisms for sail angle adjustment, including prototype testing for controlling sail size and angle. We ultimately chose to control sail size due to its relatively simple and stable mechanism. In the later stages, we incorporated a braking system for speed control in specific sections and simplified the mechanism to achieve weight reduction and maximum acceleration. Different decision-making modes were adopted at various design stages: the initial phase emphasized stability and distance, the mid-phase focused on mechanical design and turning effectiveness, and the final phase aimed at speed control and weight reduction. This phased decision-making approach ensured that the design was progressively refined and that adjustments were effectively made according to the current design goals at each stage.

Our final design showcases several advantages.

1. Firstly, using PD control for the sail angle has achieved closed-loop control, effectively reducing the impact of external disturbances and ensuring stable movement under various wind speed conditions.
2. The overall design demonstrates excellent system integration, with the mechanical structure and electronic control system highly coordinated to ensure stability and high performance.
3. Additionally, we achieved outstanding design results within a limited budget, showcasing effective cost-management capabilities.

However, there are still areas for improvement in the design.

1. First, the control system should more finely plan the expected trajectory and subdivide control sections to achieve higher precision.
2. As wind speed from the fan may vary over time, adding real-time wind speed sensors would help improve control effectiveness.
3. Additionally, the current mechanism is relatively heavy, resulting in slower acceleration and deceleration responses. Further reducing the mechanism's weight would enhance the vehicle's dynamic performance and response speed.

In conclusion, Aero Rider demonstrates our team's innovative capability and technical application level in wind-powered vehicle design. Although there is room for improvement, the overall design has met the expected goals in terms of stability, performance, and innovation, laying a solid foundation for future improvements and applications. We believe that through further research and optimization, Aero Rider will exhibit even stronger performance and competitiveness in practical applications.

## 2. Design Requirement

### 2.1 Navigation Strategy

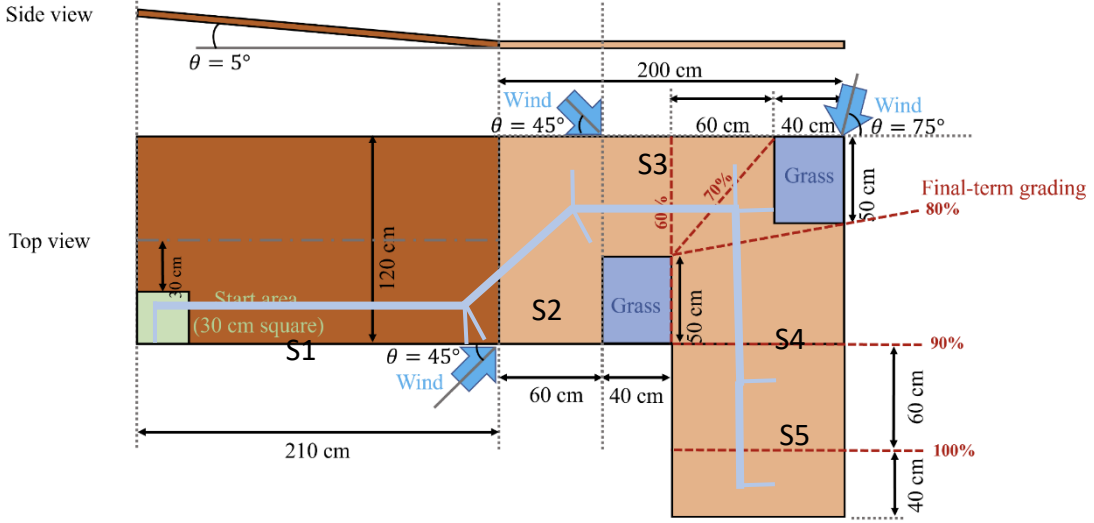


Figure 1. The ideal route for the final test

To navigate through the track, we first mapped out the ideal path and divided the route into five segments, as illustrated in the figure above. For Segment 1, we plan to use the brake to slow down the vehicle, ensuring it doesn't touch the grass. From Segment 2 to Segment 5, we will employ PD control to maintain the vehicle's heading in the desired direction. The following section will provide a detailed discussion of the control principles we implemented.

### 2.2 Working Principle for the Chassis and Brake

#### 2.2.1 Chassis

The chassis must meet these key requirements: it must be rigid and capable of supporting the lifting and sail mechanisms without any deflection, which could lead to energy loss. Additionally, it needs to accommodate the encoder wheel system and brake system, ensuring that there is sufficient space for these components without causing any interference.

#### 2.2.2 Brake

In segment 1 of the figure above, the brake system must operate. Since the grass is now UNTOUCHABLE, we need to reduce the vehicle's velocity on the slope to facilitate easier leftward movement at the fan number 1.

### 2.3 Working Principle for Control and Sail Design

#### 2.3.1 Working principle

After conducting a test run with our midterm vehicle, we observed that the final

section of the test track generates a force that pushes the vehicle off course. To address this issue, we came up with the idea of using the principles of flight controls as the basis for our control system.

In aviation, aircraft achieve the desired lift by adjusting the angle of attack of the wing. Similarly, for our vehicle, the angle of attack is determined by its yaw, or the rotation around its vertical axis. By manipulating the vehicle's yaw, we should be able to control its path and counteract the forces encountered on the test track. This approach leverages proven flight control techniques to maintain stability and ensure the vehicle remains on course.

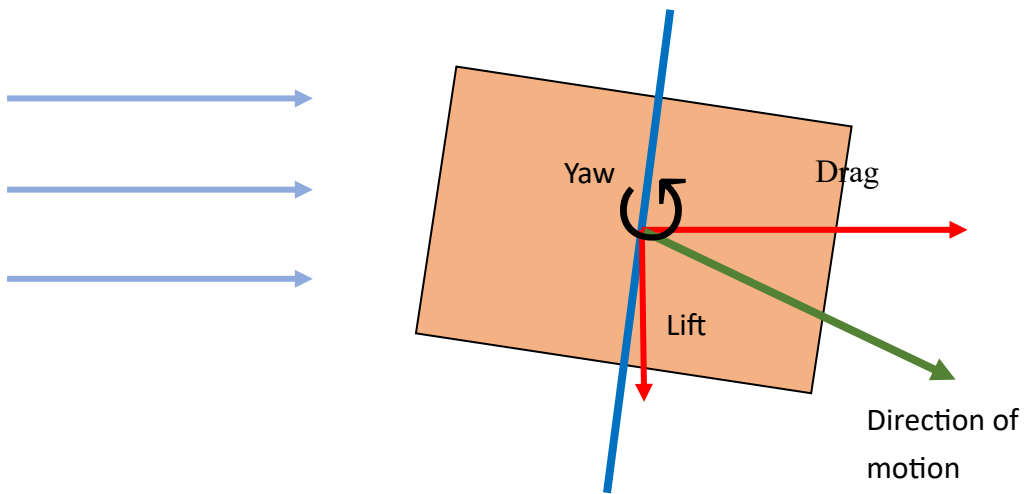


Figure 2. The free body diagram of the vehicle

To achieve this goal, we designed a sail in the shape of a half-circle, driven by two servo motors. By controlling the angle of the servo motors, we can create an uneven sail shape around the center of the vehicle. Consequently, this allows the vehicle to turn to the desired yaw value.

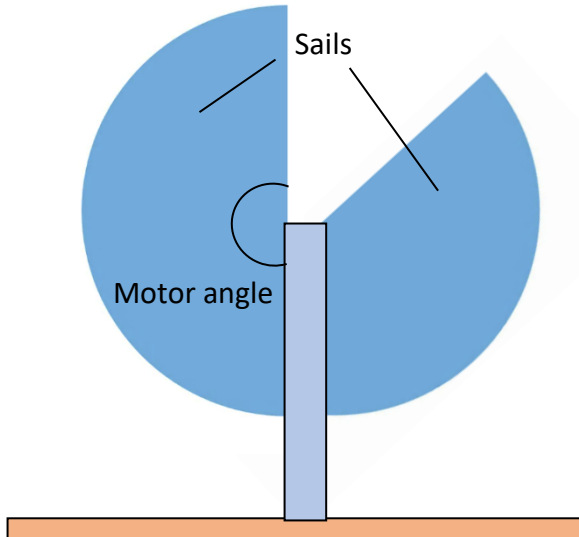
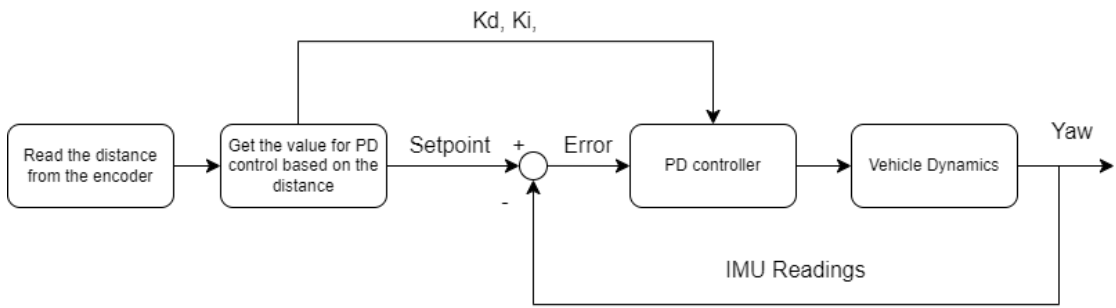


Figure 3. Simplified drawing of sail design

To achieve automatic control, we decided to use two sensors as our control feedback. The first sensor is an encoder, which measures the distance the vehicle has traveled. This allows us to determine the desired yaw value based on the encoder's reading. The second sensor is an IMU, which provides the current yaw value of the vehicle. By comparing the actual yaw value to the desired yaw value, we can determine the yaw error. We then use PD control to automatically adjust the vehicle to achieve the desired angle.

### 2.3.2 PD Control

To achieve automatic control, we developed a control method for this vehicle. The block diagram is shown below:



We write the code ourself so that the vehicle can turn to the desired angle automatically. The code we used is as shown:

```

// PID
unsigned long lastTime;
double errSum, lastErr;
double kp, ki, kd;
double lastSetpoint = 0, lastError = 0;

```

Figure 4. Global variables of the PID controls

For the global variables, we need to first construct the variable “lastTime” so that we can discretely operate the derivative and integral calculations. Next, the variable “errSum” is used for integration, which is where the integral coefficient is applied. The variable “lastErr” is used for the derivative calculation, where the derivative coefficient is applied. The variables “kp”, “ki”, and “kd” are the coefficients for the proportional, integral, and derivative terms, respectively. Lastly, “lastSetpoint” and “lastError” are initialized to zero for maintaining the previous setpoint and error values.

```

void Compute(double Input, double Setpoint, double midpoint){
    unsigned long now = millis();
    double timeChange = (double)(now-lastTime);
    double error = Setpoint-Input;
    errSum += (error*timeChange);
    double dErr = (error-lastErr)/ timeChange;
    double delta = kp*error + ki*errSum + kd*dErr;
    Output1 = midpoint + delta;
    Output2 = midpoint - delta;
    if(Output1 >150){
        Output1 = 150;
    }
    if(Output1 <0){
        Output1 = 0;
    }
    if(Output2 >150){
        Output2 = 150;
    }
    if(Output2 <0){
        Output2 = 0;
    }
    lastError = error;
    lastTime = now;
}

```

Figure 5. Functions for PID controller.

The “Compute” function is designed to maintain a desired setpoint using a PID controller. It takes three parameters: “Input”, “Setpoint”, and “midpoint”. First, the current time is stored using the “millis()” function, and the elapsed time since the last function call is calculated. The error, which is the difference between the setpoint and the input, is computed next. The integral term is updated by adding the product of the error and the elapsed time, while the derivative term is calculated as the rate of change of the error. The PID controller output is then determined by combining the proportional, integral, and derivative terms with their respective coefficients. This output is used to adjust “Output1” and “Output2” based on the “midpoint”. To ensure the outputs remain within acceptable limits, they are constrained within the range of 0 to 150 (0 is where the sail totally expanded). Finally, the previous error and time values are updated for use in the next function call.

```

void loop() {
    readIMU();
    kp = 10;
    ki = 0;
    kd = 0.2;
    Compute(yaw, 60, 0); //Compute output with input, setpoint , midpoint.
    motor5.write(Output2);
    motor6.write(Output1);
}

```

Figure 6 The code for PD control

To use the PD controller, we first need to read the yaw value using the “readIMU()” function. Next, we set the coefficients “kp”, “ki”, and “kd”. It is worth noting that because we are using PD control, the integral term coefficient “ki” is set to 0. The “Compute” function is then called with the parameters “yaw”, “setpoint”, and

“midpoint” to calculate the control outputs. Finally, the computed outputs “Output2” and “Output1” are written to “motor5” and “motor6”, respectively, using the “write” function.

### 2.3.3 Encoder Readings

We design an encoder with two degrees of freedom; therefore, it could measure the length that the vehicle has traveled. Therefore, with the reading of the IMU and the encoder, we should be able to locate where our vehicle has gone to.

### 2.3.4 Parameters

We have roughly divided the path into 5 segments. At each segment there is a corresponding value for setpoint, midpoint, Kp, and Kd. And the value we used is shown in the following table:

Table 2-1-1. Setpoint, midpoint, Kp, and Kd for each segment

Segments	Start(mm)	End(mm)	Setpoint	Midpoint	Kp	Kd
S1	0	700	Trigger the brake periodically, and raise the sail when vehicles travels 500mm from start.			
S2	700	2200	60	0	15	0.4
S3	2200	2850	-10	80	15	0.4
S4	2850	3850	-90	60	15	0.4
S5	3580	END	-90	0	15	0.4

Setpoint is the desired angle between the vehicle and the direction the slope declines, Yaw is the angle between the vehicle and direction the slope declines, midpoint is the start angle that the sails expand.

## 2.4 Working Principle for Control and Sail Design

To ensure the design meets its intended functionality, we need to validate three key parameters. The first is the effective surface area of the sail, which significantly influences the vehicle's range and acceleration in the wind field. The second is the response characteristic of the steering system, crucial for precise navigation. The third is the braking system's effectiveness, which is vital for speed control.

If conflicts arise between these parameters, the priority should be given in the following order: sail surface area, steering response characteristic, and braking ability. This prioritization aligns with the design phases outlined in the introduction, where each parameter corresponds to a specific design phase.

### 3. Design Concepts and Layout

#### 3.1 System Overview

In this section, we will go through each system that compose the whole vehicle. To achieve the desired control, we designed an integrated system that includes the sail, chassis, and braking mechanisms. We incorporated an electromechanical system to seamlessly coordinate these components, ensuring precise control and effective implementation of our control principles.

#### 3.2 Sail Deployment

##### 3.2.1 Lifting Mechanism

Our lifting mechanism employs a rack and pinion system to raise the sail to a height of 60 cm, enhancing wind capture. The key components are a 3D-printed rack, a straight bar with teeth along one side, and a 3D-printed pinion gear that meshes with the rack. The rack's end features a flat surface designed as a platform for installing the sail.

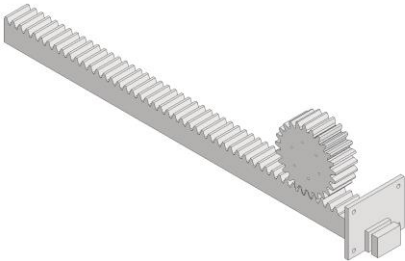


Figure 7. Rack and Pinion Design

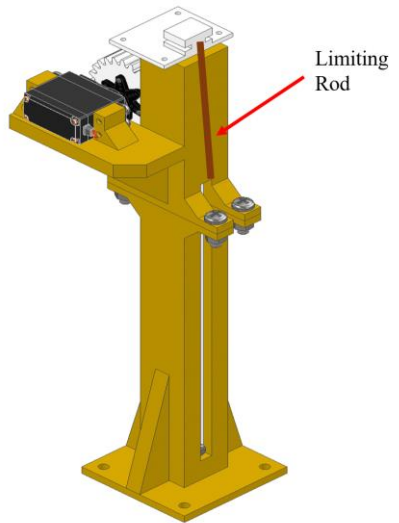


Figure 8. Lifting Mechanism's CAD

A rigid frame supports the mechanism, restricting the pinion's lateral movement and ensuring smooth, aligned motion of the rack. The frame is designed to withstand wind forces, keeping the sail stable and preventing excessive tilting or swaying when lifted.

To operate the lifting mechanism, we utilize a 360 degrees servo motor MG995[1] drives the pinion, providing sufficient torque to elevate the sail. We assign the angle of the servo motor to be over 90 degrees to rotate in counter clockwise direction for roughly 1.8 seconds to lift the rack up by 203 mm.

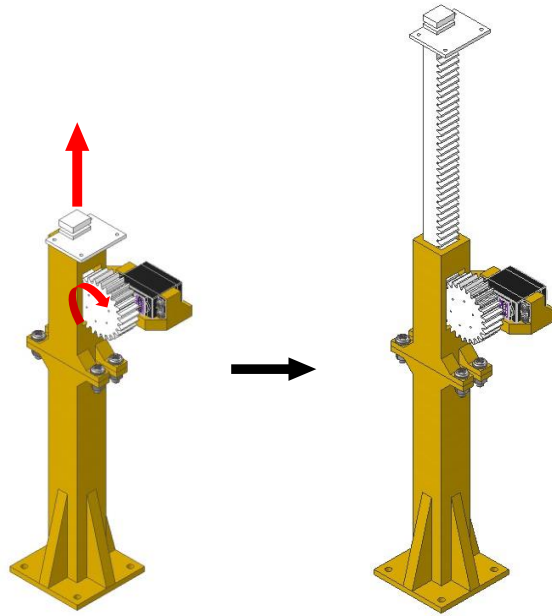


Figure 9. Operation principle of lifting mechanism

To secure the mechanism when the sail is fully raised and prevent the rack from falling, we utilize a long, thin piece of plywood as a limiting rod. This manual lock compensates for the 360-degree servo motor's inability to control the stopping angle precisely. (Figure 5)

### 3.2.2 Sail Design

We designed the sail as two 180-degree fan-shaped sails, with an MG90[2] servo motor in the middle to control the sail size. To improve stability, we decided to arrange the sails at a 150-degree angle to each other, forming a V-shape. This configuration allows for more efficient control of the vehicle's direction. The L-bracket in the end of the sail is for increasing the drag coefficient, enable the sail to generate more drag while using the same projection area.

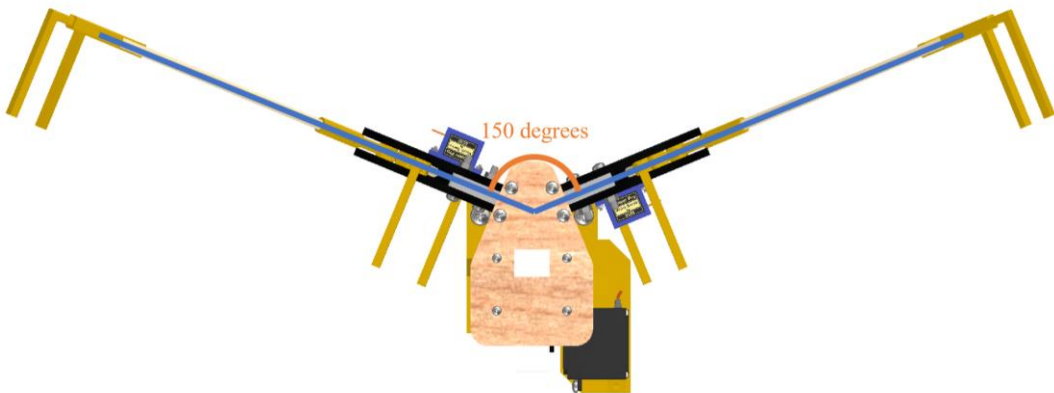


Figure 10. V-shaped Configuration

To enable the sail to expand smoothly, we design several slide rails for the frame

of the sail to move. We added some oil to reduce the roughness, making it easier for the servo motors to drive. The servo in the middle of the sail mechanism will drive the top slider and the lower slider will also be driven since they are all connected by the sails.

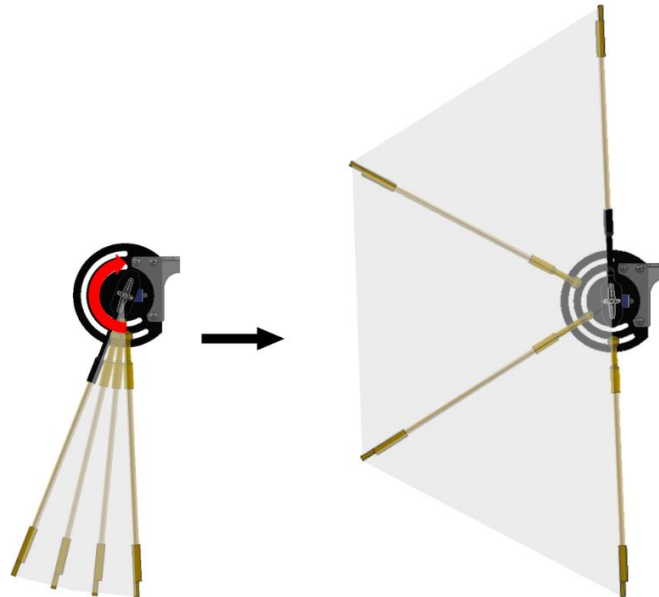


Figure 11. Operation principle of sail mechanism when fully expanded

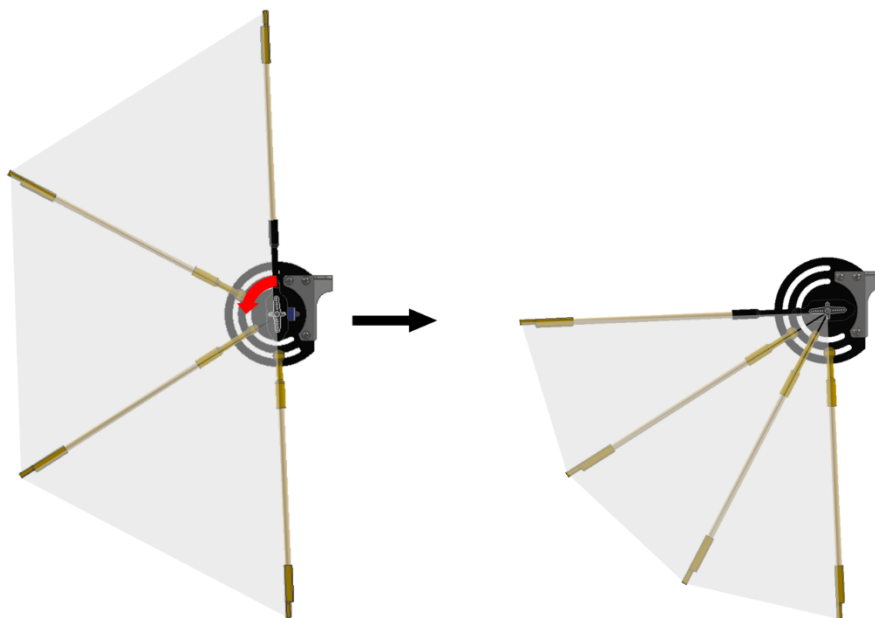


Figure 12. Operation principle of sail mechanism when half-expanded

### 3.2.3 Sail Dimension Determination

The size of the sail is determined by the ability to initiate motion when the vehicle comes to halt at the end of the flat runway. To enable the vehicle to move, it must overcome the static friction force. According to the equation:

$$f = \mu_{rolling}N$$

where  $f$  represents the static friction force,  $\mu_{rolling}$  is the rolling friction coefficient, and  $N$  is the normal load acting on the vehicle. The normal force  $N$  readily determined by placing the vehicle on a weighing scale. Given that the maximum weight for this project is 2 kilograms, we assume  $N = 2 \times 9.8 = 19.6 N$

Based on our measurement (explained in Section 4), we denote that the rolling friction coefficient  $\mu_{rolling} = 0.032$ . Therefore, the force required to initiate motion ( $F$ ) must exceed the frictional force, calculated as follows:

$$F \geq f = \mu_{rolling}N = 0.627 N$$

We can estimate the sail area needed for moving the vehicle. According to the formula of drag coefficient, we can know the projection area has a positive correlation with the Drag produced.

$$C_d = \frac{D}{1/2 \times \rho U^2 A}$$

Where  $C_d$  is drag coefficient.  $D$  is drag, which equals to the  $F$  mentioned previously.  $\rho$  is air density.  $U$  is flow speed.  $A$  is projection area. The exact dimension of the sail will be covered in section 4.

To maximize the projection area and the drag coefficient, we design the barebone of the sail to be flat and perpendicular to the ground. Additionally, to increase the wind speed caught by the sail, increase the drag coefficient, and minimize the space needed for our vehicle, we design two flat sails with L-shaped bracket to increase drag coefficient.

### 3.2.4 Energy Transfer

Let's assume we want the vehicle to turn left at fan 1. We let the sail at the right side fully expand to receive the wind, and it can be seen as a single wind beam acting on the force center of the sail.

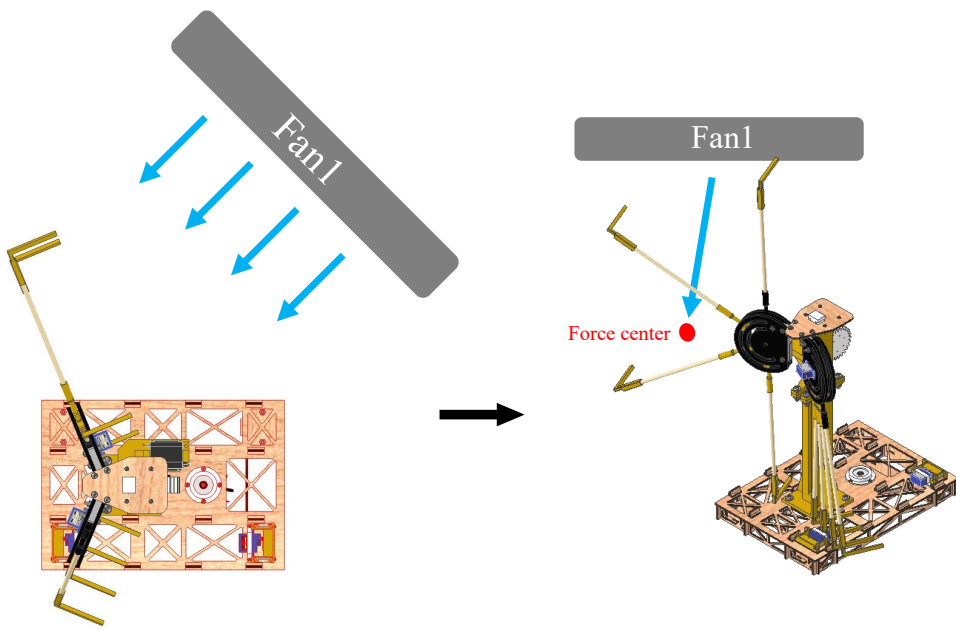


Figure 13. Indication of Force Exerting on Sail

Since the force center of the sail and the gravitational center of the vehicle are not at the same point, the force will push the vehicle forward and generate a moment counterclockwise simultaneously.

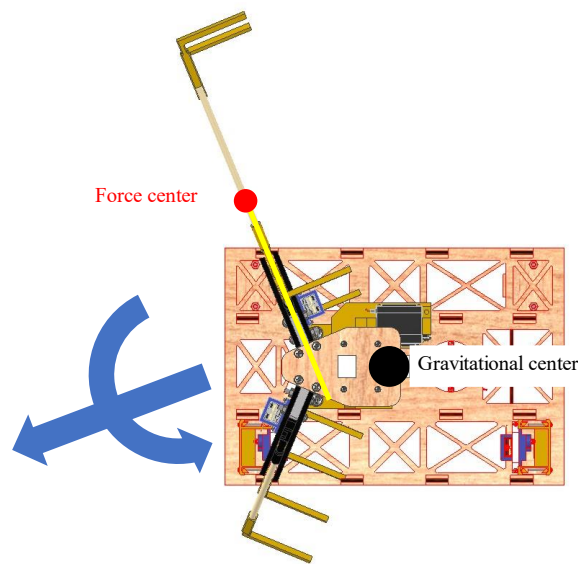


Figure 14. Vehicle Dynamics

### 3.3 Chassis Design

The initial chassis design was based on the maximum dimensions allowed by the rules, as we had not yet finalized the sail and electromechanical configurations. Our goal was to ensure the chassis could support up to 2 kilograms without deforming. To achieve this, the chassis includes multiple rib plates for enhanced structural integrity, allowing for lightweight construction without compromising strength.

We chose MDF (Medium Density Fiberboard) for the chassis due to its ease of processing and adequate mechanical properties. MDF can be precisely cut using a laser cutter, ensuring that the chassis components meet the design specifications. This material offers a good balance of strength and rigidity, essential for supporting the vehicle's load during operation without significant deformation. Using MDF as the material of the chassis not only provides the needed strength but also costs down the whole project.

The chassis was designed to the maximum allowable dimensions to maintain flexibility for future sail and electromechanical configurations. The placement and number of rib plates were determined through mechanical analysis, ensuring even stress distribution and minimizing weak points. Additionally, the rib plates' positions were carefully considered to accommodate the wheels, encoder wheels, and sail mounting points. This structural optimization enhances the chassis' overall stability and durability. The overall strength analysis is shown in the next section.

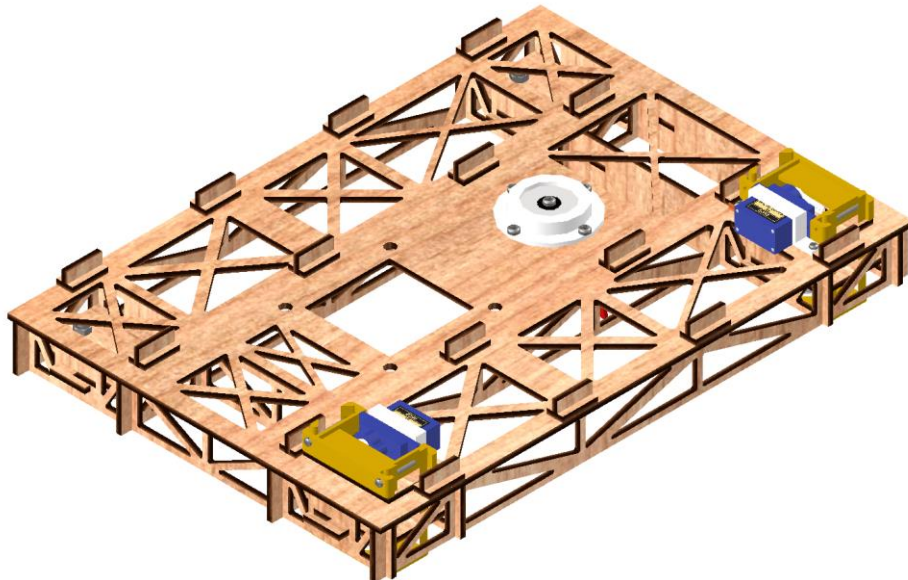


Figure 15. CAD Model of our Chassis Design

### 3.4 Design and Analysis of the Braking System

#### 3.4.1 Braking Design Logic

The purpose of the braking system design is to effectively control the deceleration of the vehicle during its operation, ensuring stability and safety. The design principle is to adjust the friction applied by the braking system on the wheels, to achieve the desired braking effect. We chose a servo motor (MG90s) to control 3D printed brake components (PLA) that press against the universal wheels (Nylon66) to reduce their rolling speed.

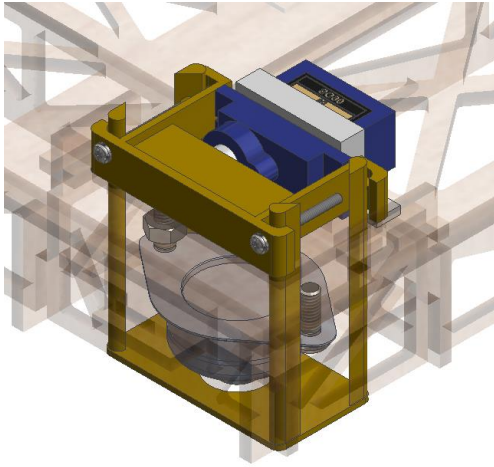


Figure 16. The braking system (Isotropic view)

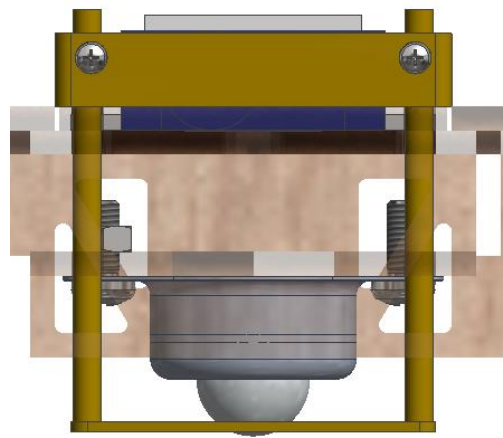


Figure 17. The braking system (Front view)

#### 3.4.2 Calculation of Braking Force

The braking force comes from both the dynamic rolling friction of the universal wheel and the braking friction.

- Friction of universal wheels: This friction comes from the rolling friction between the universal wheels and the ground, calculated as  $F_{rolling} = \mu_{rolling} \cdot N$ , where  $\mu_{rolling}$  is the coefficient of rolling friction between the universal wheels and the ground, and N is the normal force (i.e., the weight of the vehicle).
- Braking friction: This friction is applied by the braking system, calculated as  $F_{brake} = \mu_{brake} \cdot N$ , where  $\mu_{brake}$  is the coefficient of friction between the brake pad and the universal wheels. Since the braking system always stops the wheel as soon as the brake is active, the total force exerted on the vehicle can be derived as  $F_{braking} = \mu_{ground} \cdot N$ , where  $\mu_{rolling}$  is the coefficient of dynamic friction between the universal wheels and the ground.

### 3.4.3 Working Principle of Braking Friction

The braking system's friction comes from the contact between the brake pad and the universal wheels. Our braking system can only control the engagement and disengagement of the brake pad and cannot adjust the contact pressure. Therefore, we control the braking force by adjusting the duration of the brake engagement and release. The PLA material used for the brake pads has good rigidity and wear resistance, making it suitable for this application.

- Material Selection: PLA material has good rigidity and wear resistance, providing stable friction.
- Control Strategy: By adjusting the duration and frequency of brake engagement and release, we achieve different braking effects. This "pulse braking" control allows us to modulate the braking force according to the required deceleration.

### 3.4.4 Vehicle Dynamics Analysis

The vehicle dynamics analysis aims to study the impact of the braking system on the vehicle's motion behavior. The primary focus is on the braking distance and stability under different deceleration conditions. Through numerical simulation and experimental data analysis, we found that the braking system effectively controls the vehicle's deceleration and stops it within a short distance.

- Equation of Motion: According to Newton's second law, the vehicle's acceleration  $a$  is:  $F_{total} = m \cdot a$ , as  $F_{total} = mg \sin \theta - F_{friction}$ , where  $\theta$  is the angle of the runway with respect to the ground,  $F_{friction}$  is the friction force,  $m$  is the vehicle mass, and  $a$  is the vehicle acceleration.
- Deceleration Calculation: Based on the total friction force, the vehicle's deceleration is:  $a = F_{total}/m$
- Braking distance calculation: Based on the initial speed  $v_0$  and deceleration  $a$ , the braking distance  $d$  is:  $d = v_0^2/2a$

To make the vehicle as slow as possible while getting into the first corner, here we say the acceleration is almost 0, the friction force should be almost as large as  $mg \sin \theta$ . Also, since the dynamic friction is derived by  $F_{friction} = mg\mu_{ground}$ , the dynamic friction coefficient should be larger or equal to  $\sin \theta$ . While in the slope of the runway,  $\theta$  is equal to  $5^\circ$ , which implies  $\mu_{ground}$  should be larger or equal to 0.854.

### 3.5 Electromechanical System

To achieve the control principles and the functions of each component, we developed our own mechatronics system.

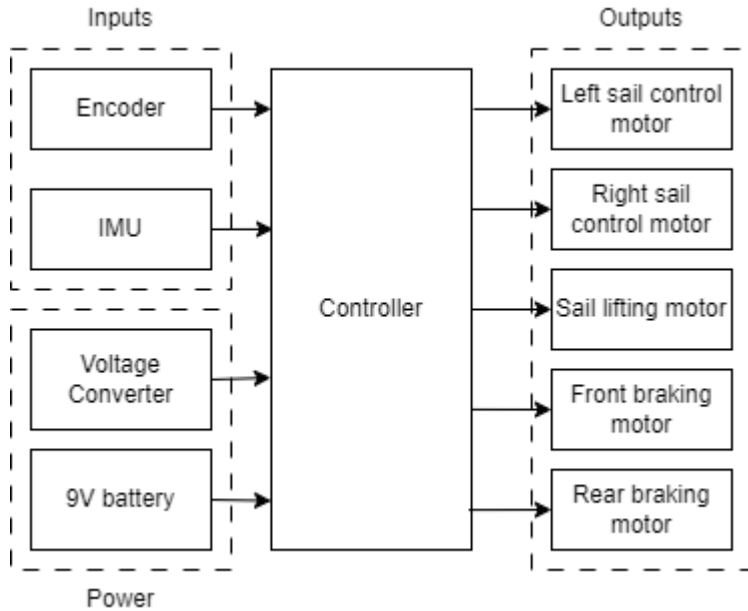


Figure 18. Mechatronics Block Diagram

#### 3.5.1 Power

In our mechatronics system, we use one MG995, and four MG90 servo motor to drive the mechanism. The maximum current of MG995 is 1.2A, and the maximum current of MG90 is 400 mA. Therefore, the voltage converter[3] should be able to produce the current more than 2.8A. We choose the ADIO-DC36V5A voltage converter, which can generate a maximum current of 5A



Figure 19. ADIO-DC36V5A voltage converter

Due to the large current drain by the servo motor, we need to power the Arduino independently. Therefore, we power the Arduino with a 9-volt battery through the DC jack.

### 3.5.2 Inputs

#### 1. Encoder:

We designed our own encoder based on the needs of our vehicle. Due to the slope, the encoder requires suspension, or it will fail at the boundary of the slope. Additionally, the encoder should have two degrees of freedom to avoid affecting the moving direction of the vehicle.

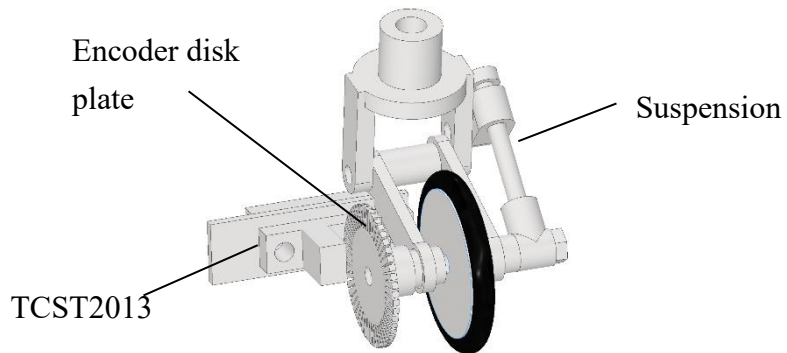


Figure 20. Design of the encoder.

The sensor we used for the encoder is the TCST2013 Transmissive Optical Sensor[4]. According to the data sheet, the turn-on time is about  $10 \mu s$ , and the turn-off time is about  $8 \mu s$ . Assume the vehicle runs at a speed of 3m/s, and the wheel diameter is 30mm, the revolutions per second (rev/s) is calculated as follows:

$$\frac{3}{0.03 \times \pi} = 31.83 \text{ (rev/s).}$$

The maximum slots of the encoder disk plate can be calculated as:

$$\text{Maximum slots} = \frac{1}{31.83 \times \text{max turn-on time} + \text{turn-off time}} = \frac{1}{31.83 \times 1.8 \times 10^{-5}} =$$

1745.38. However, due to the nozzle size of 3d printer, the maximum numbers of slots we can produce is 50 slots.

#### 2. IMU:

To obtain the vehicle's yaw, we use an Inertial Measurement Unit (IMU), specifically the MPU-6050. The MPU-6050 is a widely used sensor that combines a 3-axis gyroscope and a 3-axis accelerometer on a single chip. This allows it to measure both rotational and linear motion.

According to the datasheet, the MPU-6050 has a maximum output data rate of 1000 Hz, meaning it can provide up to 1000 data points per second. This high data rate ensures accurate and timely measurements of the vehicle's yaw, which is crucial for

precise control and navigation.

### 3.5.3 Outputs

#### 1. Sail Motors

The weight of the sail is 0.041 grams, and its length is 30 cm. Assuming the sail is a homogeneous rod, the maximum torque needed to drive the sail is:

$$0.041 \times \frac{30}{2} = 0.615 \text{ kg} \cdot \text{cm}.$$
 From the datasheet, the stall torque of the MG90 ranges

between  $1.8 \text{ kg} \cdot \text{cm}$  and  $2.2 \text{ kg} \cdot \text{cm}$ , which more than sufficient to drive the sail.

#### 2. Lifting Motor

To lift the sails quickly, we need a motor with sufficient strength. A higher torque results in faster sail elevation. Therefore, we chose the MG995 servo motor, as it provides the highest torque available within our budget constraints. This motor is not only powerful but also cost-effective, making it an ideal choice for our design.

## 3.6 Vehicle System

To sum up, the primary design requirements for the Aero Rider vehicle include maintaining dimensions within 30cm x 21cm x 40cm and a weight limit of 3kg. The vehicle must be constructed within a budget of NTD 3000, with all components integrated by the team. It needs to autonomously deploy its sails, achieve the longest possible distance within 3 minutes, and avoid obstacles.

To easily raise the sail, we utilized a rack and pinion mechanism to generate greater force, supported by a rigid frame that ensures the pinion can fully transmit power to lift the mechanism. To control the vehicle's direction by changing the sail size, we use two servos. To prevent singularity points during control, the sails are arranged at a 150-degree angle to each other. Additionally, an L-bracket at the end increases the drag coefficient, enabling the sail to produce more drag with the same projection area.

The chassis uses multiple rib plates to enhance structural strength while reducing the vehicle's weight. Through mechanical analysis and optimization, the chassis is designed to be both lightweight and strong. The braking system is designed with calculated friction to ensure effective speed control.

For the PD controller, we use two sensors to provide feedback: an IMU and an encoder. The electromechanical system must include these two sensors. The encoder design includes a suspension to prevent failure at the boundary of the slope. Motor selection is based on the specific requirements of each mechanism.

With these design requirements, the vehicle is then tested and optimized to meet these needs and pass the final test.

## 4. Analysis and Verification

### 4.1 Rolling Friction of the Universal Wheel

From section 3.3.2, we have concluded that the friction force without braking is by dynamic rolling friction. The rolling friction can be derived by

$$F_{rolling} = \mu_{rolling} \cdot N$$

, where  $\mu_{rolling}$  is the coefficient of rolling friction between the universal wheels and the ground and  $N$  is the normal force (i.e., the weight of the vehicle).

To derive the rolling friction  $\mu_{rolling}$ , there are some parameters we have to be careful of, which are the normal force, the diameter of the sphere, the velocity, the material, and the roughness.

From the Elastic Compression Calculator[5] from NIST (National Institute of Standards and Technology), which is based on the research by M.J. Puttock and E.G. Thwaite[6], the deformation when weight is equal to 2 kg is 10.124  $\mu\text{m}$ . The deformation is much smaller than the ball's diameter, 15.875 mm. Since the rolling friction is mainly formed by the displacement of the sphere, we assume that if the normal force is under 2 kg, the rolling friction coefficient is independent of the normal force.

The research by Rod Cross[7] concluded that the rolling friction is dependent of the diameter of the sphere and the velocity. Another research also done by Rod Cross [8] shows that the rolling friction is dependent of the material and the roughness.

To determine the rolling friction exerted on the wheels, and thus the vehicle, we designed an experiment to measure it. The working principle of the experiment device shown in Figure 21 is that the universal and weight would be moving in a circular path; hence, there will be a centripetal force. Because of the friction, the driven link would have an angle between the radius of the circular movement (as shown in Figure 22). Therefore, we can derive the friction force with the angle and the centripetal force.

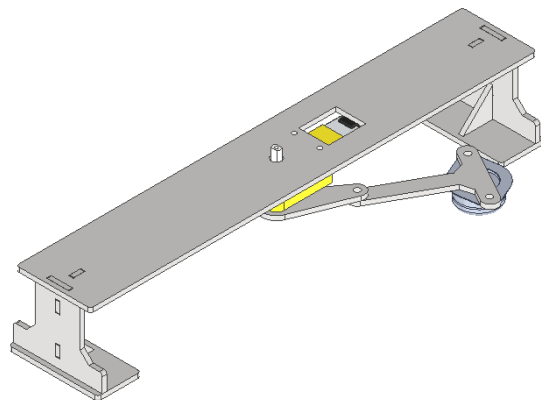


Figure 21. Experiment Setup (Isometric view)

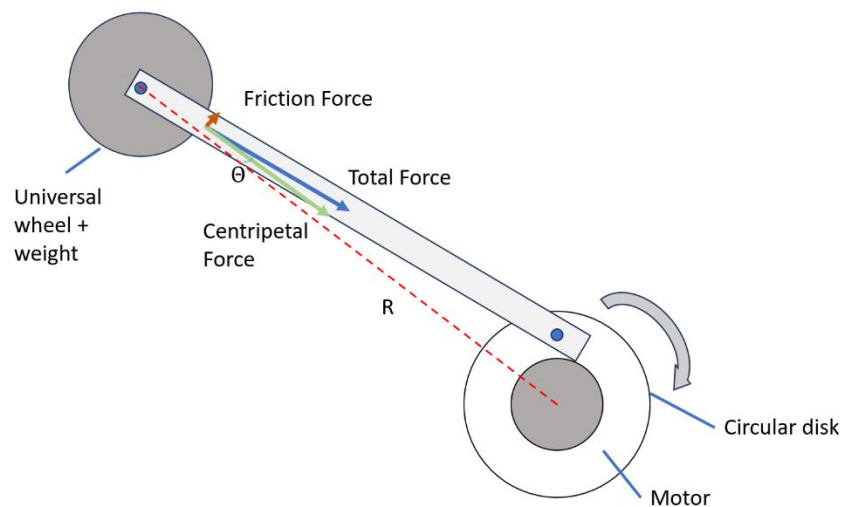


Figure 22. The forces with our experiment device (the size is not to scale)

The centripetal force is derived with the equation  $F_c = m \frac{V^2}{R}$ , where R and V can be measured through a camera. Therefore, we can calculate the Friction F with the equation  $F_f = F_c \tan\theta$  where  $\theta$  is also measured through the camera.

The components used in the experiment are as shown:

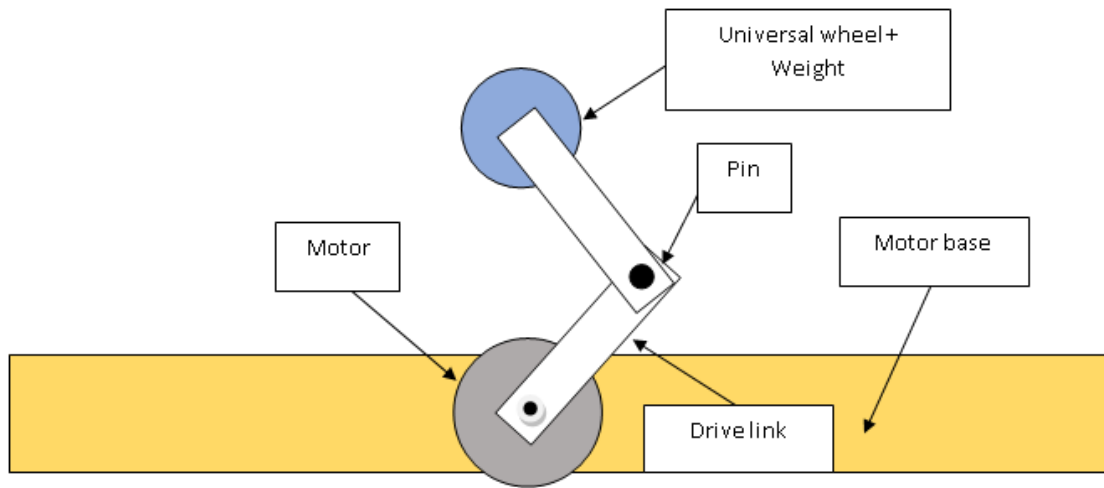


Figure 23. Experiment Setup (top view)

1. Motor: The motor is driven in different with different voltages so that it can produce different speeds.
2. Motor base: The motor base is used to secure the motor.
3. Pin: The pin can freely rotate so produce no moment on the universal wheel.
4. Drive link: The drive link is used to pull the universal wheel and weight.

We use the software “Tracker” to measure the velocity of the universal wheel, the radius of the movement, and the angle between the driven link and the radius of the movement. The measurement is done as shown in Figure 24. The weight of the universal wheel and weight is 189g.

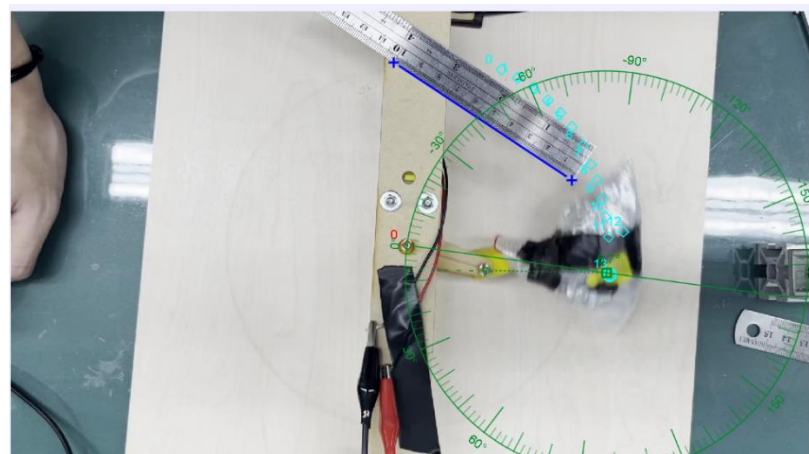


Figure 24. The measuring picture of Tracker

Table 1. Measurement Data of the experiment

theta	R(m)	omega(rad/s)	V(m/s)	F(N)	friction(N)	mu
6.5	9.67E-02	-5.55E+00	5.36E-01	5.62E-01	6.40E-02	0.0345346
8.8	9.34E-02	-4.07E+00	3.80E-01	2.93E-01	4.53E-02	0.0244468
10.8	9.35E-02	-2.90E+00	2.71E-01	1.48E-01	2.83E-02	0.0152498
5.6	9.66E-02	-7.12E+00	6.88E-01	9.26E-01	9.08E-02	0.0489709
6.7	9.58E-02	-5.69E+00	5.45E-01	5.87E-01	6.89E-02	0.0371647

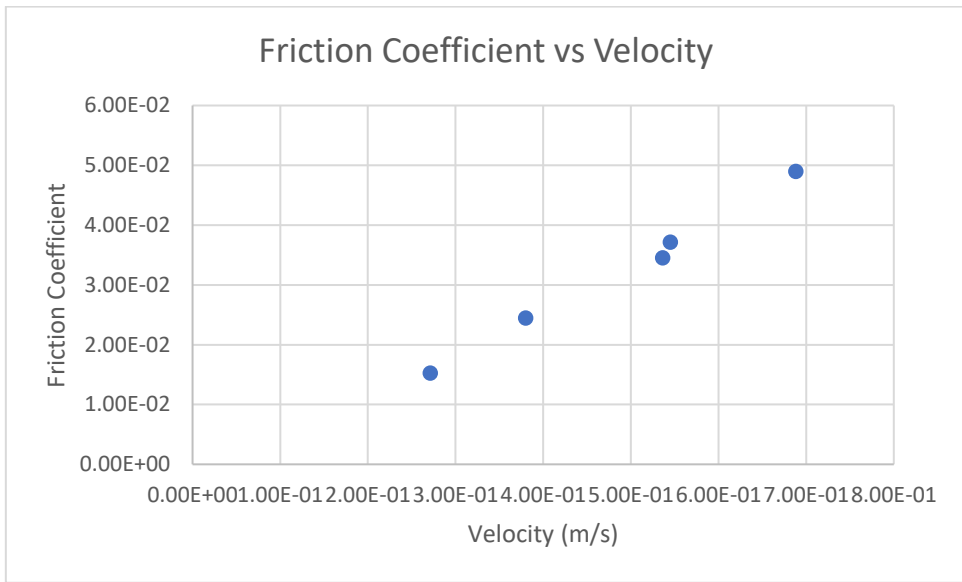


Figure 25. Friction Coefficient vs Velocity.

It is shown that the rolling friction coefficient is about linear to the velocity increases, the tendency is almost the same as other materials we found in the papers. [7]

## 4.2 Sail Analysis

### 4.2.1 Theoretical Analysis

Assume the temperature is  $20^{\circ}\text{C}$ , then  $\rho = 1.204 \text{ kg/m}^3$ . From previous calculation,  $D = 0.627 / \cos(15^{\circ}) = 0.649$  for half of the sail.

Our goal is to make sure the vehicle can move even when the wind is weak. By observation, the lowest wind speed occurs at the end of the runway, which is about the 90 points mark line. From direct measurement, the wind speed is about  $2 \text{ m/s}$ .

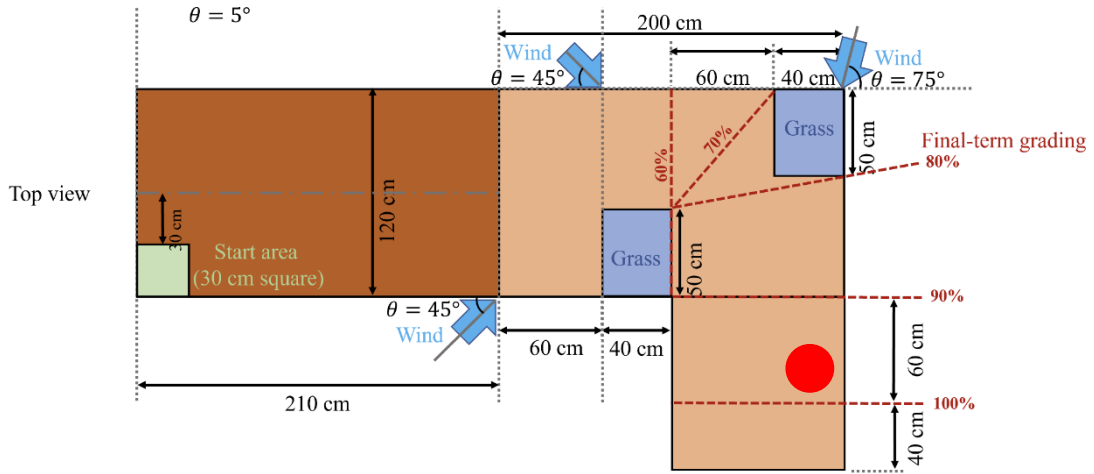


Figure 26. Low wind speed area (red point)

For the drag coefficient, we know that the plastic sail will at least be flat during operation. Thus,  $C_d = 1.28$  (Drag coefficient for flat plate) is the lower bound for our sail. From the drag coefficient formula mentioned earlier, we can derive the area needed for moving the vehicle forward.

$$A = \frac{D}{1/2 \times \rho U^2 C_d} = \frac{0.649}{1/2 \times 1.204 \times 2^2 \times 1.28} = 0.211 m^2$$

$$R = \left(\frac{A}{\pi}\right)^{0.5} = 0.259 m$$

Consequently, the radius of our sail is designed to be  $0.28 m$  each. In theory, the drag we produced is:

$$D = 1/2 \times \rho U^2 C_d \times A = 0.76N$$

$$F_{total} = D \times \cos(15) = 0.733N > 0.627N$$

We use upper bound for vehicle weight, lower bound for drag coefficient and air speed. Consequently, our vehicle will perform better than theoretical acceleration, which we have the confidence that the vehicle can move even if it stop.

#### 4.2.2 Design Verification

Utilizing the force sensing module provided by the teaching assistant, we measured the drag produced by the entire vehicle. Due to differences between the measuring environment and our initial estimates, we noted that the wind speed was approximately 3.3 m/s at the location marked by the red point in Figure 26.

Theoretically, the drag produced by the sail was calculated to be 1.996 N. However, the measured force was approximately 2.104 N, which is 5.4% higher than our estimate.

This discrepancy can be attributed to our conservative design, particularly the addition of an L-shaped bracket that increased the overall drag coefficient. Additionally, the higher ambient temperature at the time of measurement contributed to the variance.

Assuming the temperature was 25°C, the air density would be approximately 1.19 kg/m<sup>3</sup>. Considering this, and attributing the error to the increased drag coefficient, we can calculate the actual drag coefficient of our sail.

$$C_d = \frac{D}{\frac{1}{2} \times \rho U^2 A} = \frac{2.104}{0.5 \times 1.19 \times 3.3^2 \times 0.28^2 \pi \times \cos(15^\circ)} = 1.36$$

### 4.3 Brake Analysis

To make the universal wheel stop spinning, we found that the force exerted from the PLA brake pad to the wheel should be larger than 1.0 kgf by experiments.

As mentioned in section 3.3.2, the total friction force between the ground and the wheel can be derived as  $F_{braking} = \mu_{ground} \cdot N$  since the wheel is not rolling during braking. With the same experiment device and method used in section 4.3.1, the measurement data of the dynamic friction coefficient are shown in Table 4-3-2-1.

Table 2. Measurement Data of the experiment.

theta	R(m)	omega(rad/s)	V(m/s)	F(N)	friction(N)	mu
3.17E+01	9.62E-02	-5.21E+00	5.01E-01	3.13E+00	1.61E+00	1.37E-01
4.26E+01	9.45E-02	-4.34E+00	4.10E-01	2.14E+00	1.64E+00	1.39E-01
7.33E+01	9.53E-02	-2.23E+00	2.13E-01	5.69E-01	1.58E+00	1.34E-01
2.02E+01	9.62E-02	-6.53E+00	6.28E-01	4.92E+00	1.51E+00	1.28E-01
3.73E+01	9.59E-02	-4.78E+00	4.58E-01	2.63E+00	1.67E+00	1.42E-01

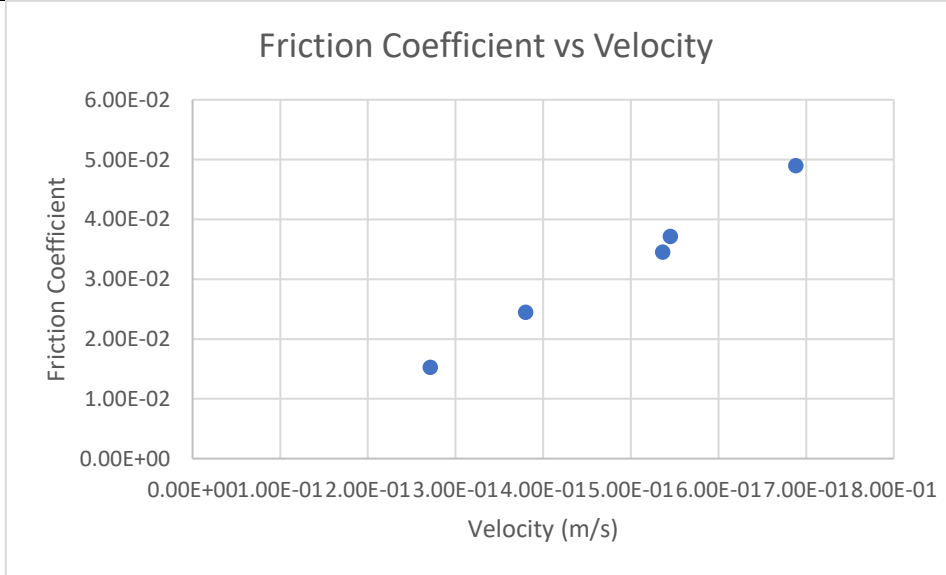


Figure 27. Friction Coefficient vs Velocity

It is shown that the dynamic friction coefficient  $\mu_{ground}$  is about constant 0.136 with velocity increase. As derived in section 3.3.4, the dynamic friction is possible to make the vehicle stop in front of the end of the slope.

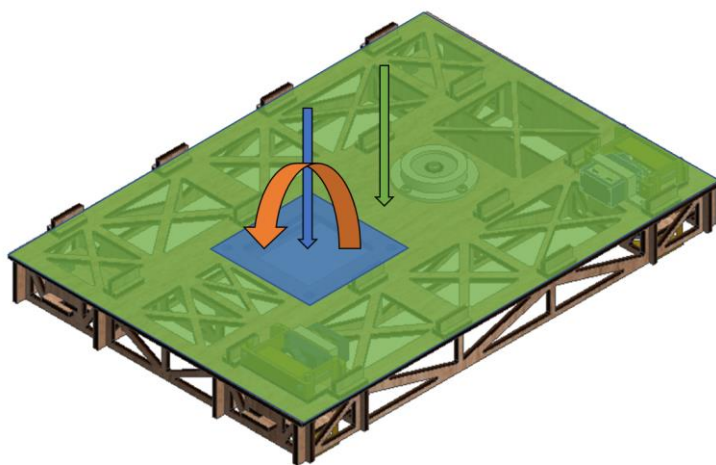
## 4.4 Chassis Analysis

We conducted a finite element analysis (FEA) to simulate the chassis' stress distribution under various loads. This analysis helped us determine the optimal rib plate arrangement, balancing structural strength with weight reduction.

### 4.4.1 Static Analysis

Evaluating the chassis' stress and deformation under static loads to ensure it can support the vehicle's weight.

- Simulation Engine: Autodesk Inventor
- Boundary Condition:



1. Blue Area: 1kgf load, represents the weight of the sail and the lifting mechanism.
  2. Green area: 1kgf load, represents the weight of electromechanical system parts uniformly exerted on
  3. Orange moment: 0.81Nm torque exerted by the sails while the height is 55cm higher than the chassis and 1.5N drag on the sails.
  4. Frictionless supports on all universal wheels.
- Simulation Results
    1. Vons Mises Stress

The below Figure 27 and Figure 28 are the stress analysis results for the chassis before and after design. The original chassis design is made by a flat plane and the new chassis is made by a plate and multiple ribs under it. The Vons Mises stress before and after design is 1.192 and 3.277 MPa respectively, with are far from the ultimate tensile stress of MDF, which is 18 MPa.

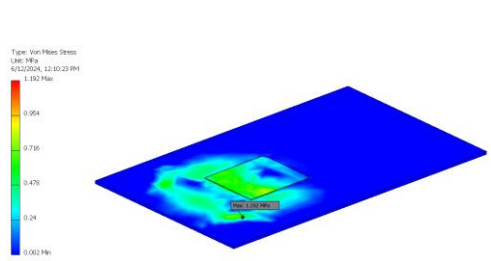


Figure 28. Stress analysis of the chassis without design.

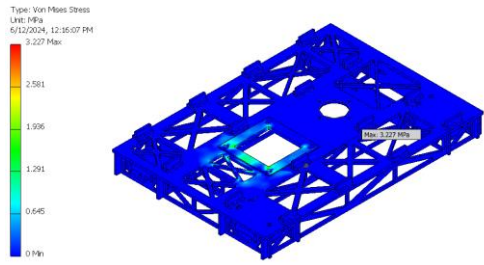


Figure 29. Stress analysis of the chassis after design.

## 2. Displacement

The below Figure 29 and Figure 30 are the displacement analysis results for the chassis before and after design. The displacement is 0.05 and 0.04 mm respectively. The designed chassis has a lower displacement under the specific load.

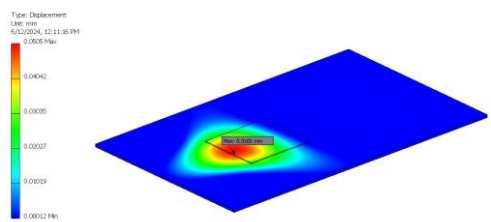


Figure 30. Displacement of the chassis without design.

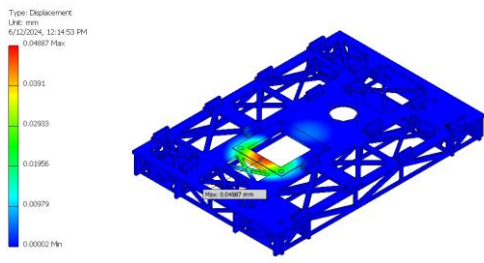


Figure 31. Displacement of the chassis after design.

In summary, our chassis design has undergone thorough mechanical analysis and multiple iterations to ensure a balance of strength, stability, and lightweight construction. Using MDF and laser cutting has proven effective, providing precision and reliability. Continuous optimization will further improve the design, supporting better vehicle performance in competitions.

## 4.5 Dynamic response of the mechatronics system

In the previous chapter, it was shown that the response time of the input sensor is so small that it is negligible compared to other components. The most critical component in the vehicle is the servo motor that controls the size of the sails. The response time of the motor directly affects the vehicle dynamics.

To measure the response time of the motor, we set up an experiment. We programmed the servo to move from 0 to 180 degrees and hold for 2 seconds. Then, we had the servo move from 180 to 0 degrees. We used a phone camera to capture the footage and analyzed the response time using software “Tracker”.

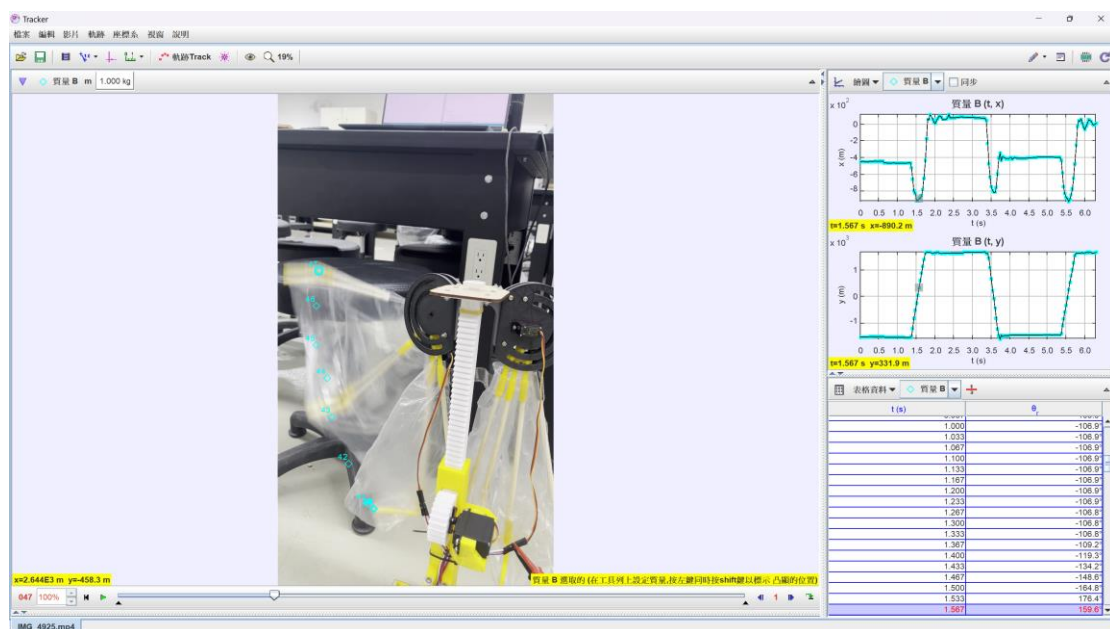


Figure 32. Tracking the position of the sail tip using “Tracker”

In Figure 31, we used Tracker to track the position of the sail tip. The expanding response time of the sail servo motor is illustrated in Figure 32. The data shows that the rise time when the sail is expanding is approximately 0.32 seconds. This rise time represents the time taken for the sail to move from 10% to 90% of its full range.

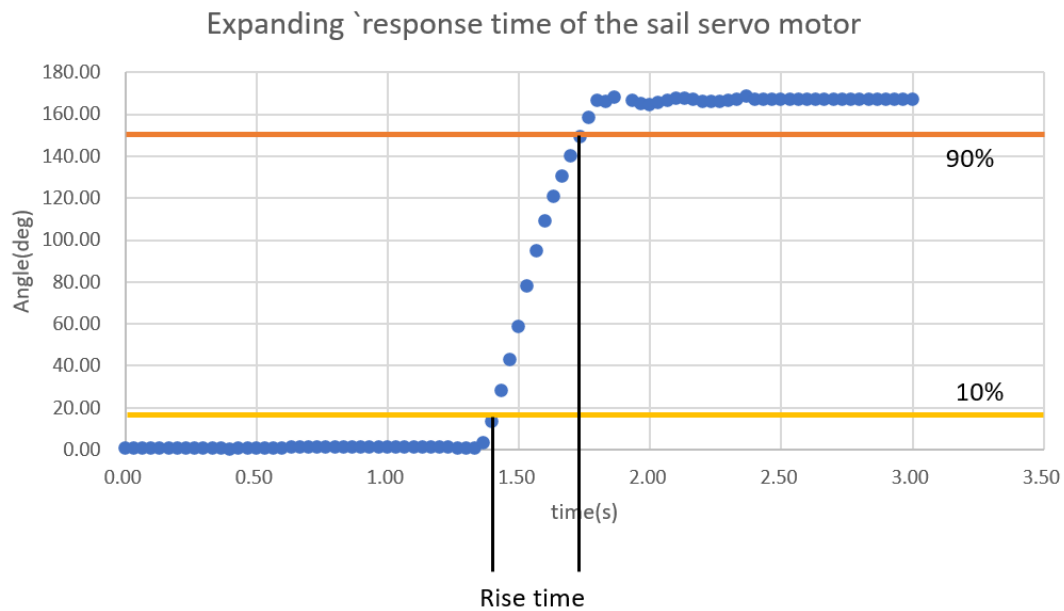


Figure 33. The expanding response time of the sail servo motor

In Figure 33, the closing response time of the sail servo motor is displayed. From the experiment, we found that the response time for the sail to close is about 0.233 seconds. Similar to the expanding response time, this measurement reflects the time taken for the sail to move from 90% to 10% of its full range.

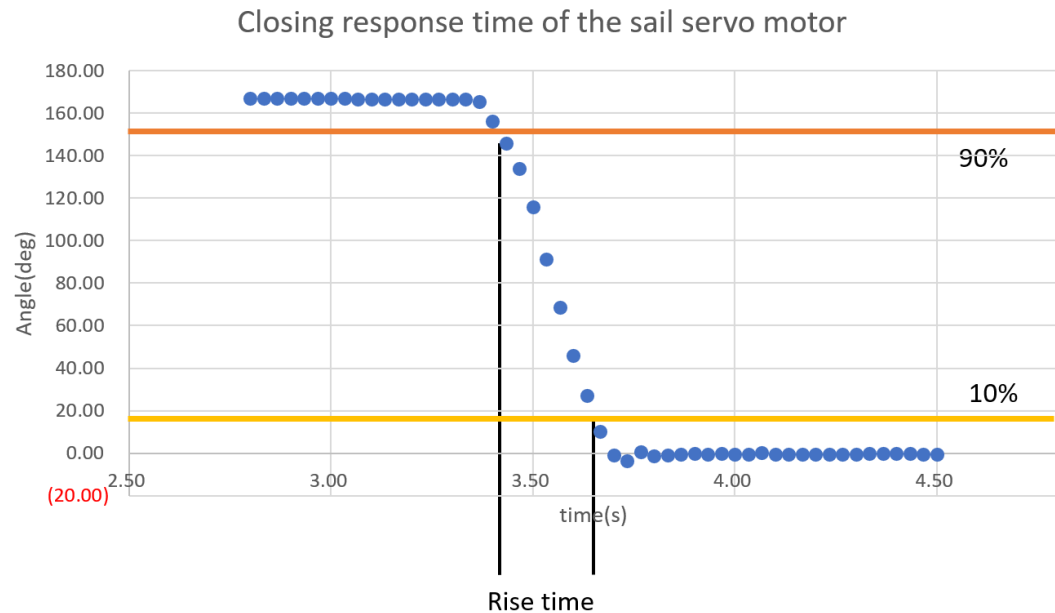


Figure 34. Closing response time of the sail servo motor

## 4.6 Dynamic response of the Vehicle

An experiment is conducted to test the steering response of the whole system. Moreover, the PID controller parameters are tuned by the experiment result.

The experiment setup:

Fix the vehicle using the bearing of the encoder wheel to constrain the degree of freedom to only rotation. Place them about 70 cm away from the nozzle of the fan. The distance is measured using the axis of rotation. To reduce the disturbance, we shut down the first two fans on the field leaving only the last one. The vehicle will be tested with different target angles and PID parameters.

The experiment step:

1. Place the vehicle parallel to the fan.
2. Initiate the onboard controller.
3. Record the whole process from above.
4. Repeat steps 1~3 for different angle targets and PID parameters.
5. Analyze the resulting video using Tracker.

Analysis process:

The orientation of the vehicle is monitored and measured by Tracker. We stick a yellow dot on the top of the sail frame to make the auto-tracking process easier and more precise. Take the bearing used to fix the vehicle as the origin, and track the yellow dot. By changing the coordinate from Cartesian to polar, the orientation is automatically calculated. Afterward, export the data to Matlab and use the stepinfo function to get the response characteristics, like rise time and percentage overshoot.

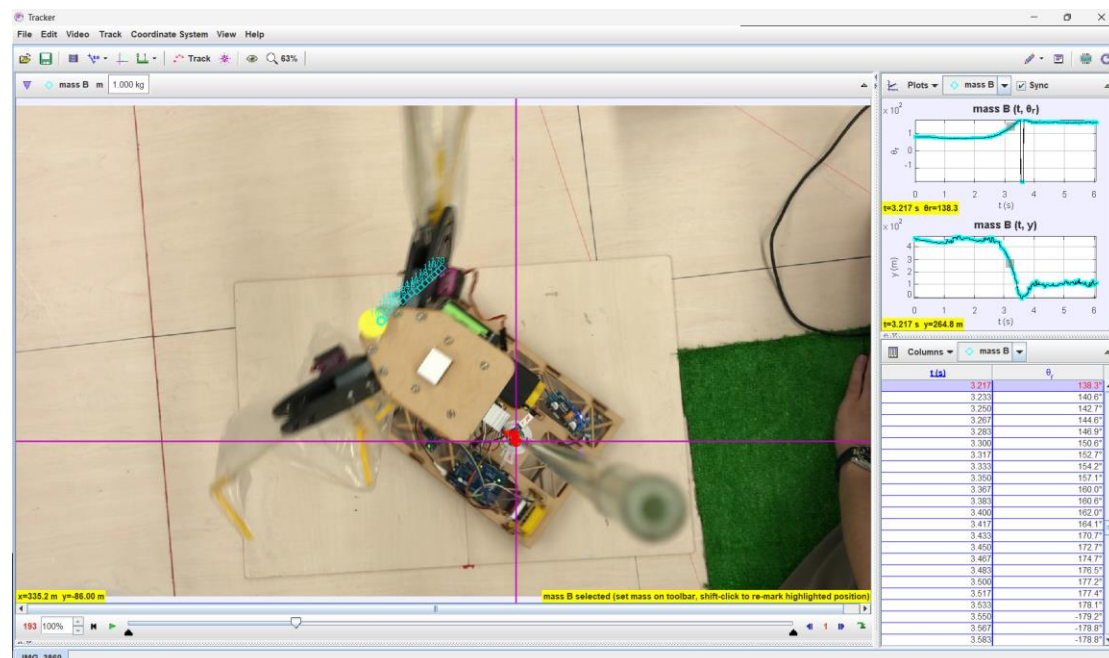


Figure 35 Experimenting using Tracker

The screenshot shows the MATLAB R2023b interface. The Editor window displays a script named 'PID\_response.m' with the following code:

```

1 % read data
2 data = readtable('實驗.xlsx', 'Sheet', '90deg');
3 head(data);
4 time = data(1:275, 'Var9');
5 response = data(4:275, 'Var11');
6
7 % calculate the response characteristics
8 info = stepinfo(response, time);
9 rise_time = info.RiseTime;
10 settling_time = info.SettlingTime;
11 overshoot = info.Overshoot;
12
13 % show response characteristics
14 fprintf('Rise Time: %f\n', rise_time);
15 fprintf('Settling Time: %f\n', settling_time);
16 fprintf('Overshoot: %f\n', overshoot);
17
18 % plot
19 plot(time, response);
20 xlabel('Time (s)');
21 ylabel('Response (\theta)');
22 title('System Response of kP 15, kD 0.4');
23 grid on;
24

```

The Command Window below shows the output of the script:

Name	Value
data	427x11 table
info	1x1 struct
overshoot	20.1163
response	272x1 double
rise_time	0.7930
settling_time	8.8627
time	272x1 double

Below the Command Window, the results are summarized:

- Rise Time: 0.793027
- Settling Time: 8.862657
- Overshoot: 20.116279

Figure 36. Analyzing using Matlab

The experiment is conducted with 3 different target angles 90, 60, and 30, and with 3 different sets of K<sub>p</sub>, K<sub>d</sub> values. The total nine results are shown below:

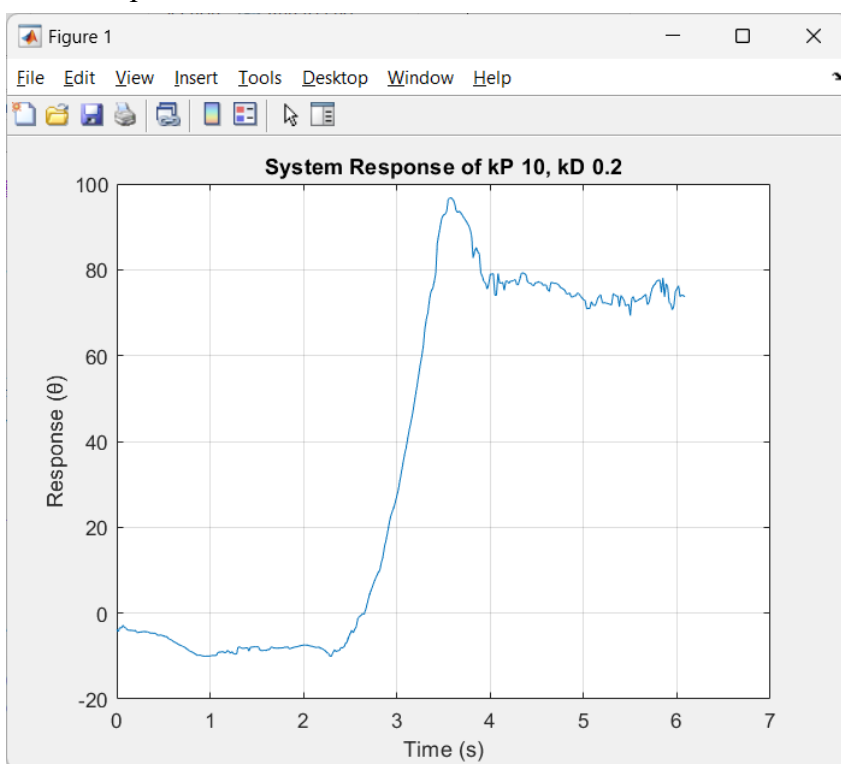


Figure 37. K<sub>p</sub>=10, K<sub>d</sub>=0.2, Set point=90

Rise Time: 0.541901

Overshoot: 31.383078

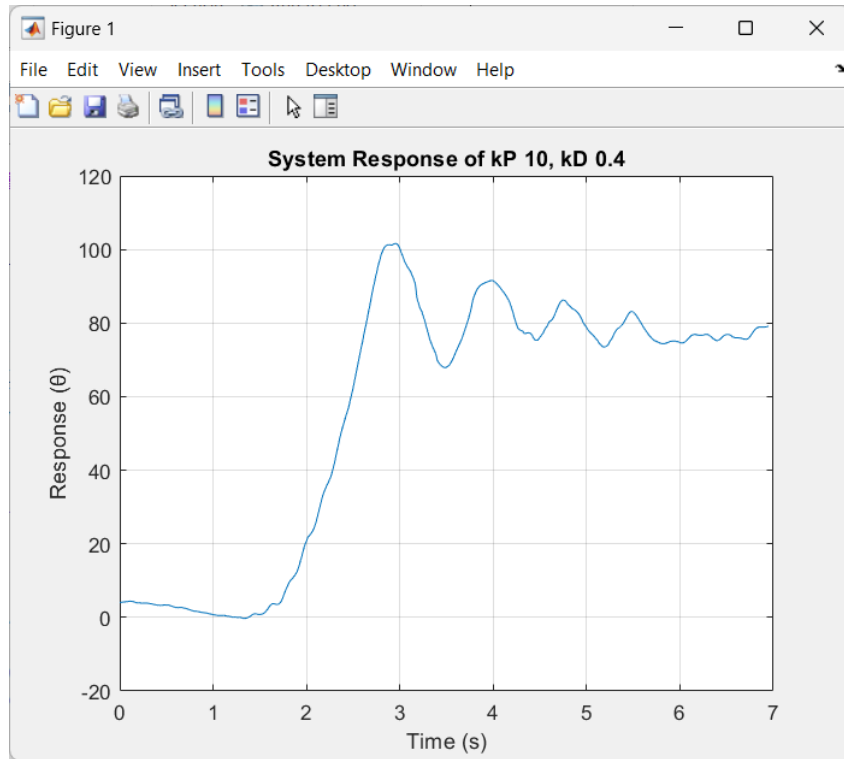


Figure 38.  $K_p=10$ ,  $K_d=0.4$ , Set point=90

Rise Time: 0.784023

Overshoot: 28.282828

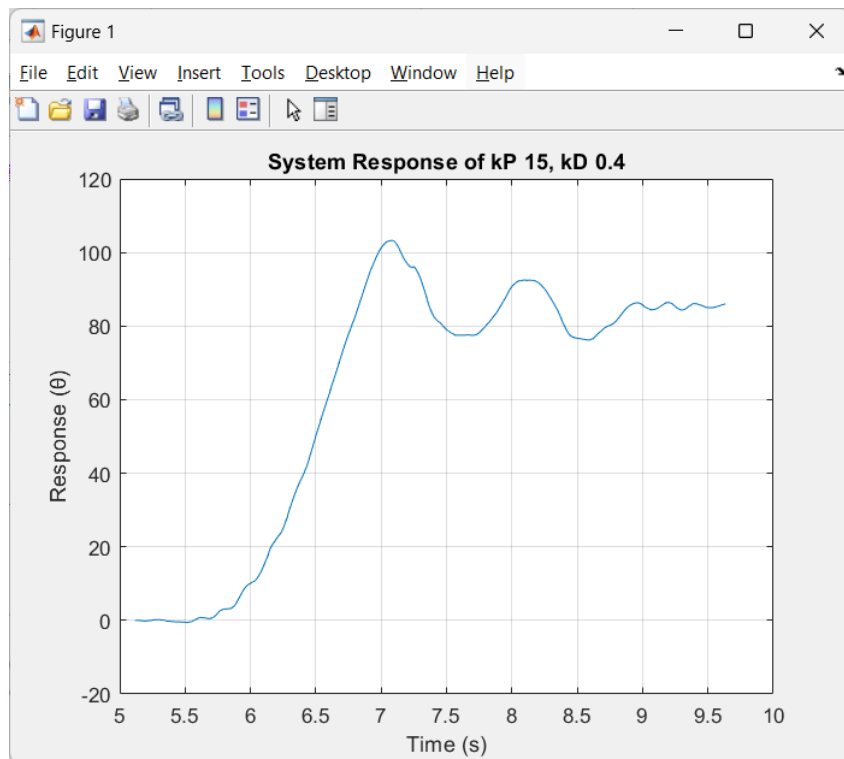


Figure 39.  $K_p=15$ ,  $K_d=0.4$ , Set point=90

Rise Time: 0.793027

Overshoot: 20.116279

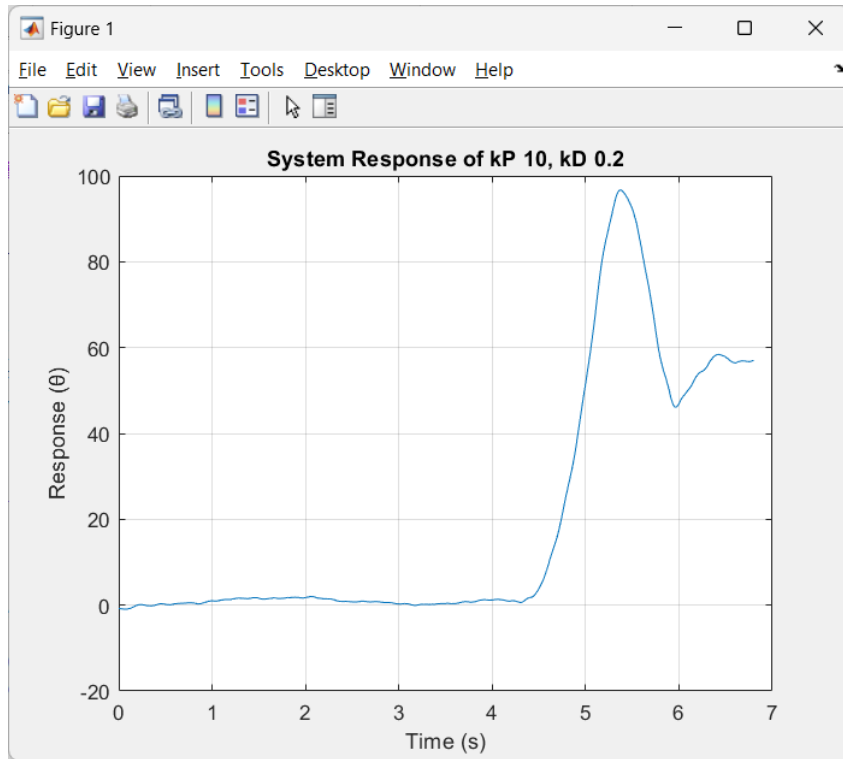


Figure 40. Kp=10, Kd=0.2, Set point=60

Rise Time: 0.632311

Overshoot: 19.678715

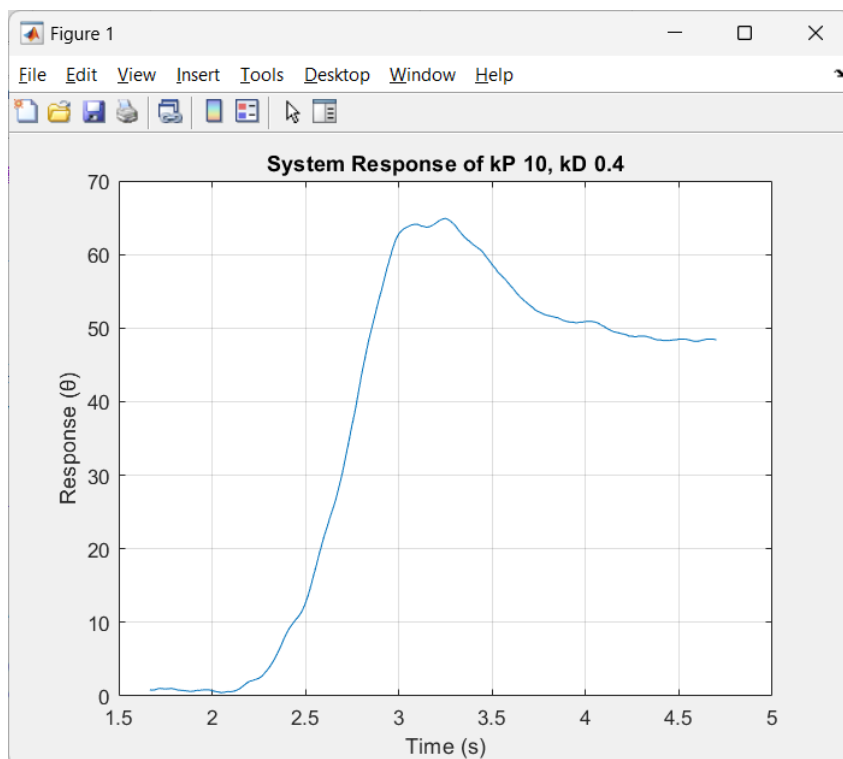


Figure 41. Kp=10, Kd=0.4, Set point=60

Rise Time: 0.469775

Overshoot: 34.090909

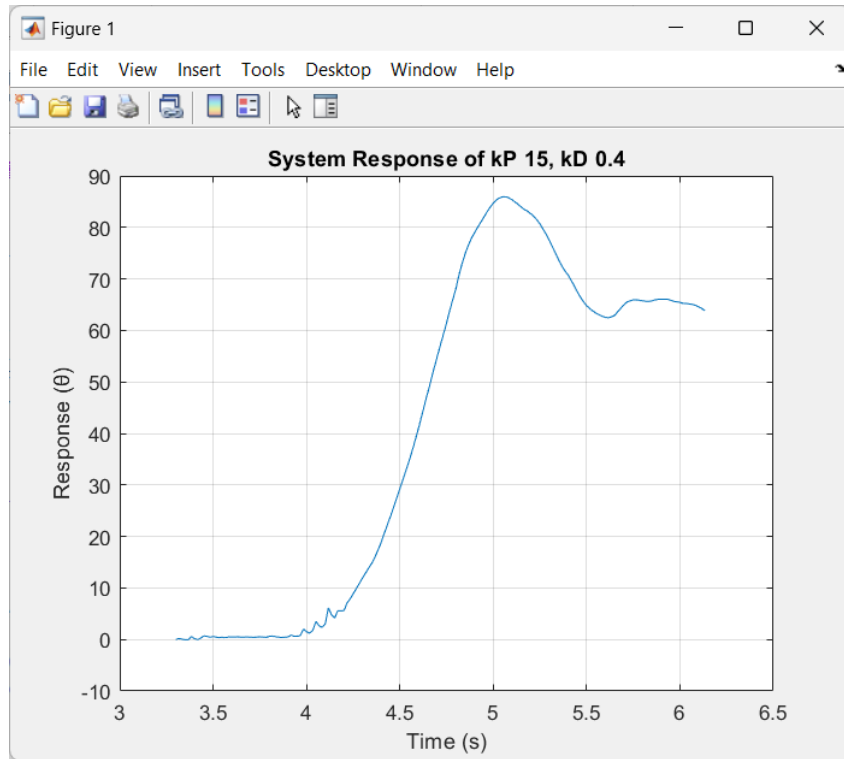


Figure 42.  $K_p=15$ ,  $K_d=0.4$ , Set point=60

Rise Time: 0.509791

Overshoot: 34.617794

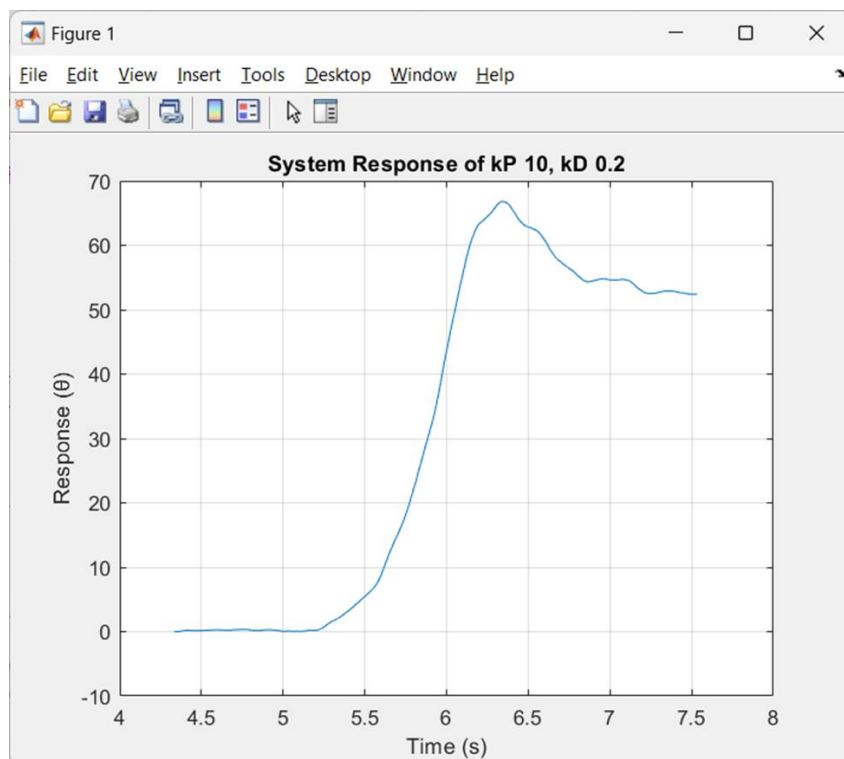
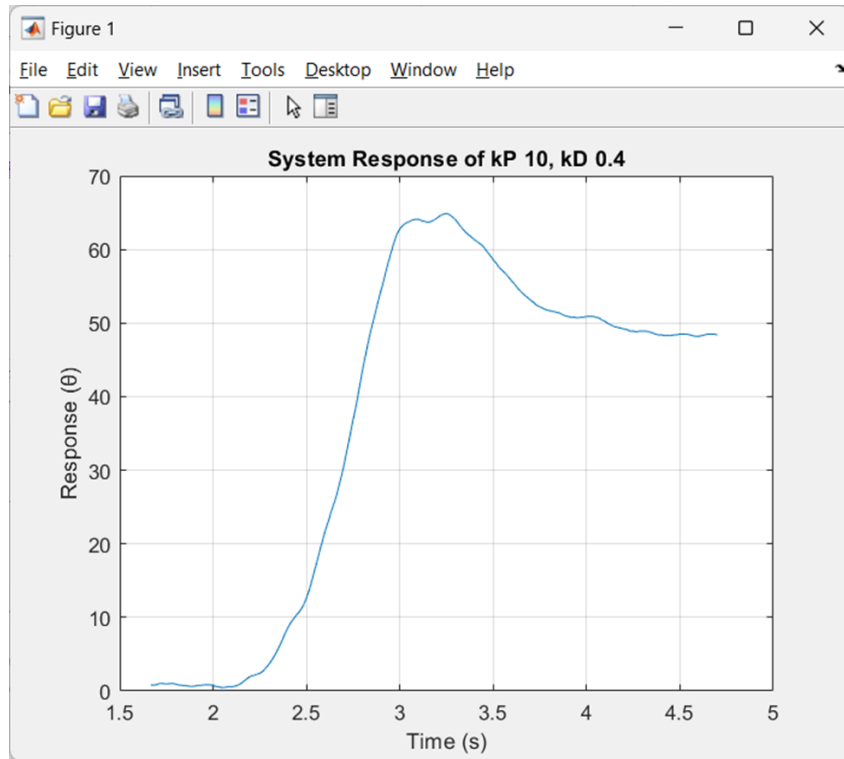


Figure 43.  $K_p=10$ ,  $K_d=0.2$ , Set point=30

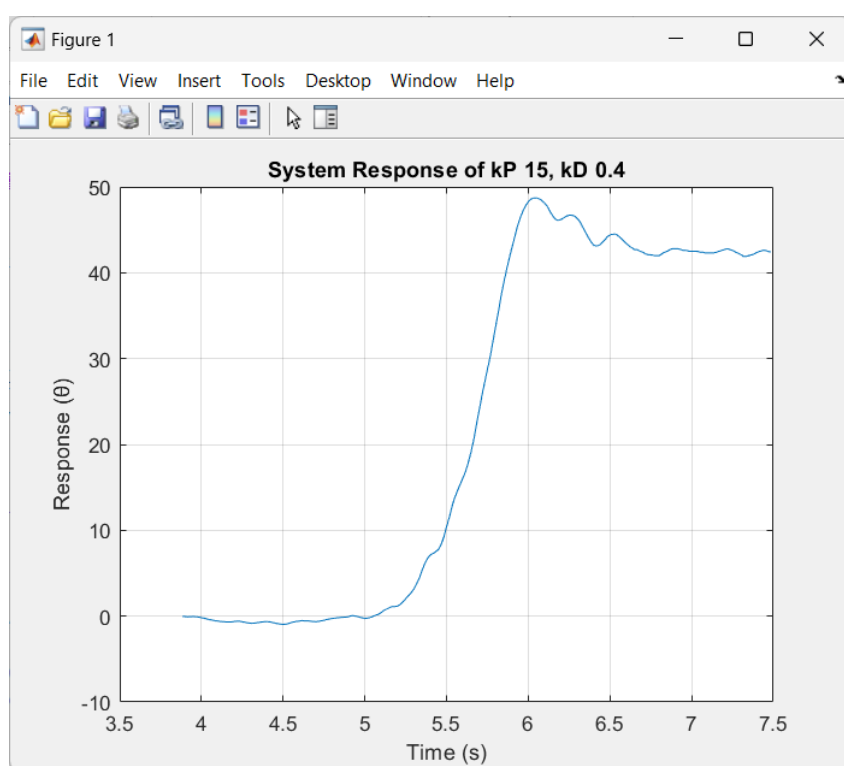
Rise Time: 0.538048

Overshoot: 27.480916



Rise Time: 0.469775

Overshoot: 34.090909



Rise Time: 0.514558

Overshoot: 14.858491

Table 3. Rise time at different conditions

target/(kP, kD)	(10, 0.2)	(10,0.4)	(15, 0.4)
90	0.54	0.78	0.79
60	0.45	0.63	0.51
30	0.53	0.47	0.51
average	0.5	0.63	0.6

Table 4. Percent overshoot at different conditions

target/(kP, kD)	(10, 0.2)	(10,0.4)	(15, 0.4)
90	31.38	28.28	20.12
60	69.65	19.68	34.62
30	27.48	34.09	14.86
average	42.83667	27.35	23.2

Two response characteristics are considered the most important factors in the overall system performance. Rise time can tell us how quickly the vehicle can turn, which corresponds to the yaw velocity. Percent overshoot will greatly affect how stable the system is. By increasing the value of Kp, the rise time can be reduced, shorter the response time of the signal to actual vehicle behavior. However, increasing Kp also has a negative effect on other properties. To cancel the instability brought by Kp, Kd should be increased. From the result shown above, we have to decide which one is more important to us. Finding the balance between yaw velocity and system stability is a tricky problem, but considering that the whole project is driven by wind provided by the field and no other power source or steering is allowed, we should make the whole system more stable. There are two reasons that made this conclusion. First, controlling the vehicle riding in a complex wind field means an overshoot may cause the sail to enter another wind flow that is not designed to be. Without other power source or steering means once an overshoot happens, it is unlikely that it will ever be able to recover. Second, avoiding touching the grass area will be the major target, an overshoot will increase the risk of the wheel accidentally touching the grass. The low yaw velocity can be compromised by reducing the vehicle speed using brakes. For the final decision, since there is little difference in rise time, we chose the one with the lowest percent overshoot, which is Kp = 15, Kd = 0.4.

## 5. Working Norms and Consensus

### 5.1 Team Contract

- Team Goals:
  - get 100 points in the 2 tests
  - be happy
  - have a sense of accomplishment after the project
  - make sure the balance between work and life
  - improve the skill of problem-solving
  - reports will be written in English
- Regular meeting time: 10-12 am every Sunday @ntume makerspace
  - may have more meetings during the design stage
- Working method:
  - every member works about 8 hours a week for this project
  - never be late 7.5min after the meeting starts
  - progress report at the start of the meeting
  - discuss before chat
  - major decisions through discussion, minor decisions through majority vote
  - have consensus after arguments
  - test for design
  - if we find the work cannot be completed, notify others 2 days before the next meeting
  - the internal deadline is 2 days before the actual deadline (team homework)
  - take turns summarizing and rewriting meeting minutes in English
- Punishments:
  - late for the meeting: \$50 snacks for each participant
  - late for submitting work results w/o valid reasons:
    - summarize and rewrite the meeting minutes in English before the next member submits work results late

## 5.2 Gantt Chart of our Work Schedule and Some Reflection

		W3	W4	W5	W6	W7	W8	W9
Concept and Research								
<b>Flywheel</b>	Construct							
<b>Sail</b>	Flow Field							
	Measuremen t							
	Area testing							
	Design							
	Construct							
<b>Chassis</b>	Design							
	Construct							
<b>Software</b>	Code							
Test and modify								
		W10	W11	W12	W13	W14	W15	W16
Concept and Research								
<b>Sail</b>	Flow Field							
	Measuremen t							
	Design							
	Construct							
<b>Chassis</b>	Design							
	Construct							
<b>Software</b>	Controller							
Test and modify								

Before the mid-term testing, our progress was in line with our expectations. However, after the mid-term test, the changeover to the new venue was slower than anticipated, and the layout underwent significant modifications. Our misunderstanding of the final test rules led to further setbacks as we had to rework certain aspects of our project to comply with the correct guidelines. Thus, we decided to postpone the schedule for one week.

Moreover, the unexpected need to design and integrate a braking system was a significant hurdle. The technical difficulties and the learning curve associated with this task were greater than we had anticipated. This unexpected addition required extensive testing and multiple iterations to ensure it met the necessary standards.

Overall, these factors combined to extend our timeline by approximately two

weeks beyond our original plan. The slower transition to the new venue, the major layout changes, and the unforeseen complexity of adding a braking system all contributed to the delays in our project's final schedule.

### 5.3 Work Distribution

C.H. Chou	J.K. Tsai	P.Y. Chang	Y.P. Chang	T.J. Wang
Lifting mechanism	Lifting mechanism	Chassis	Sail-opening mechanism	Lifting mechanism
	Lifting mechanism			IMU code
Test and modify				
Braking mechanism	Lifting mechanism	Chassis	Lifting mechanism	Sail-opening mechanism
	Sail-opening mechanism	Controller		
		Code		
Test and modify				

### 5.4 Peer Review

#### 5.4.1 Evaluation Criteria

##### 1. Participation

- o 1 point: Rarely participates in group activities and discussions, minimal contribution.
- o 2 points: Low participation, occasionally absent or not engaged.
- o 3 points: Average participation, attends most activities and discussions.
- o 4 points: Actively participates in group activities and discussions, good engagement.
- o 5 points: Very actively participates in all activities and discussions, outstanding contribution.

##### 2. Contribution

- o 1 point: Almost no substantial contribution, minimal work done.
- o 2 points: Low contribution, only completed a small portion of work.
- o 3 points: Average contribution, completed assigned tasks.
- o 4 points: Good contribution, completed own tasks and assisted others.
- o 5 points: Outstanding contribution, not only completed own tasks but also

provided valuable suggestions and helped others.

### 3. Collaboration

- o 1 point: Hardly collaborates with others, negative attitude.
- o 2 points: Poor collaboration skills, sometimes difficult to work with.
- o 3 points: Average collaboration, able to work with team members.
- o 4 points: Good collaboration, works well with others and communicates effectively.
- o 5 points: Excellent collaboration, proactively coordinates group work and resolves conflicts.

### 4. Creativity

- o 1 point: Lacks creative thinking, no new ideas proposed.
- o 2 points: Low creativity, only a few new ideas suggested.
- o 3 points: Average creativity, proposes some constructive suggestions.
- o 4 points: Good creativity, offers multiple valuable innovative ideas.
- o 5 points: Exceptional creativity, frequently proposes innovative solutions that significantly benefit the project.

### 5. Responsibility

- o 1 point: Lacks responsibility, often delays or fails to complete work.
- o 2 points: Low responsibility, sometimes delays or fails to complete work.
- o 3 points: Average responsibility, completes assigned work on time.
- o 4 points: Good responsibility, completes work ahead of schedule and with high quality.
- o 5 points: Excellent responsibility, always completes work ahead of time, high quality, and willingly takes on extra tasks.

#### 5.4.2 Evaluation Results

	C.H. Chou	J.K. Tsai	P.Y. Chang	Y.P. Chang	T.J. Wang
<b>Participation</b>	5	5	5	5	5
<b>Contribution</b>	5	5	5	5	5
<b>Collaboration</b>	5	5	5	5	5
<b>Creativity</b>	5	5	5	5	5
<b>Responsibility</b>	5	5	5	5	5
<b>Total Score</b>	25	25	25	25	25

## 6. Personal Reflection and Suggestions

B10502021 周知穎

Initially, I think the concept of this course is pretty nice. Being able to use all the things that we learned throughout the three years is a great way to mark a period to the learning in mechanical engineering. Everything was fine before the midterm testing, the instructions are clear and there is enough time for development with the easy challenge.

After the midterm, we immediately started to discuss the new design and changes to make, but later it was all a waste of time because of the regulation changes. The final version being set just six weeks before the actual test. The difficulty of the final challenge was significantly higher than the midterm, but due to changes in the venue and rules, the preparation time was delayed. For example, the rule changed from allowing the vehicle to run over the grass to prohibiting any contact with it. I believe these changes impacted many students' progress.

Additionally, the teaching assistants did not conduct thorough and complete tests of the final exam setup, leading to unclear difficulty levels. The concept behind the final exam was to have students use wind fields to control the sails, making the vehicle turn without hitting the grass. Our team aimed to achieve this by controlling the sail areas on both sides.

We discovered that adding numerous control methods made it even harder for our vehicle to perform perfectly on the track. Due to the instability of the generated wind, controlling the vehicle in such a variable environment proved to be very challenging.

Despite these difficulties, I learned a lot throughout this class. This was my first time leading a team, and while we had worked together before, everyone had their own preferences. Managing such a talented group was not easy, but it was rewarding to see so many different ideas emerge during our brainstorming sessions. Deciding on the final concepts was challenging, as we spent a lot of time discussing and debating everyone's thoughts.

This experience of having thorough discussions and evaluating various ideas was unique. Unlike other teams, our main problem was having too many ideas and finding it difficult to identify flaws in multiple concepts. This led us to develop a complicated system. Despite these challenges, we managed to work through all the difficulties.

Although we didn't achieve our desired result in the final testing, I want to express my gratitude: "Thank you, everyone, for your effort and time. We really have done a great job!"

B10502039 張伯宇

I believe the testing items in this course might be its biggest issue. I think the professors hope students can analyze problems from an engineering perspective and try to design an engineering project based on their own analysis. However, in this midterm test, I noticed that the control aspect was significantly overlooked. Because the operation was manual, the task was simply to measure how many seconds the sail would take to unfurl after being released. Furthermore, the uncontrollable factors of the Buehler wheel created too much unfairness in this course. In the experiment for the midterm report, we tried to change the weight distribution of the car, hoping to alter the performance of the Buehler wheel. However, the results showed that no matter how we adjusted the weight, the variability among the Buehler wheels dominated the car's dynamics. These wheels' characteristics were also heavily affected by dust and other factors, making it highly likely that the car design would fail during the test.

For the final test, aside from the setup issues that prevented much of the work from being completed in advance, the rules were constantly changing. The teaching assistants also hadn't conducted test runs beforehand, so many of us students had to act as the first batch of guinea pigs. Besides the grassy areas, some sections of the field were affected by fans blowing in opposite directions. If the car got caught in these areas, it would become uncontrollable, requiring it to pass through using its inertia. This made the feasible paths even narrower than the ones surrounded by grass. Even though we tried to use control mechanisms to complete the challenge, the differences in fan effects between the two fields were too significant. The successful paths were so narrow that it was impossible to use a single control theory effectively. We had to spend long hours adjusting to the specific conditions of each field. Many students stayed up all night in the workshop a day or two before the test, trying to find suitable parameters to adapt to each field.

I believe a course should allow students to spend more time thinking, giving them more opportunities to identify the root causes of the outcomes and solve them. However, the overall result was that the uncertainties greatly exceeded the feasible paths planned by the instructors. Based on the response time under our PD control, the car needed to maintain a certain speed to pass through wind-free areas using inertia. However, before reaching a steady state, the car was forced into the next segment of the path, leaving us to make constant, minute adjustments. These unstable factors were far greater than what control mechanisms could suppress.

Therefore, I think this course needs more time for the teaching assistants to validate the fields, ensuring that both sides are not only theoretically consistent but also practically identical. Regarding the issues with the Buehler wheels and the fans, I believe their disturbances are too significant, with uncontrollable factors outweighing

controllable ones. To improve, perhaps the scale of the practical course should be increased. For example, enlarging the field size, increasing the weight of the car, and using stronger winds could make the controllable factors more significant than the uncontrollable ones. This way, students can see the aspects they can adjust and make scientifically based modifications, rather than relying on luck as in the midterm Buehler wheel lottery and the final practical statistics.

B10502063 張曜鵬

This mechanical engineering practical course has been immensely fulfilling, providing a hands-on experience that has significantly deepened my understanding. Throughout the project of building a small car, I have acquired valuable skills and insights that are not easily attainable through theoretical studies alone.

One of the most enriching aspects of this course was the opportunity to apply theoretical knowledge in a real-world context. Working on the project allowed us to encounter and solve practical engineering problems, enhancing our problem-solving skills and creativity. The collaborative nature of the project also fostered a strong sense of teamwork and communication among team members, which are essential skills in any engineering career.

The new project topic was particularly exciting and offered a fresh challenge that kept us engaged and motivated. Each step, from the initial design to the final testing, was a learning experience that contributed to our overall growth as budding engineers. While the course was highly beneficial, there were a few areas where I believe improvements could enhance the learning experience further. For instance, the change of the testing venue after the midterm evaluation occurred too late, which affected our preparation time. Additionally, the adjustments to the fan angle were made too slowly, further reducing our available time for practical testing towards the end of the course. Another recommendation is to record the first lecture where the rules and guidelines are explained. This would help prevent any misunderstandings between students and instructors, ensuring everyone has a clear and consistent understanding of the project requirements from the beginning.

When writing this final report, I understand the car's characteristics more after organizing the experiment data and results, including the vehicle dynamic and the PD parameter adjustments. Therefore, I think it would be beneficial to publish the report's structure earlier in the course. Encouraging students to think about the required experiments for the report during the project development phase would provide a clearer direction for their design process and reduce the burden of writing the report at the end of the term.

Furthermore, allowing students to choose certain aspects of the final report or to submit bi-weekly progress reports could offer a more flexible and engaging way of documenting their progress. This approach might lead to more thoughtful and detailed experimentation and ultimately result in better learning outcomes for future students.

Overall, this course has been an invaluable part of my education, blending theoretical knowledge with practical application. The insights gained and the skills developed throughout this project will undoubtedly serve as a solid foundation for my future endeavors in mechanical engineering. By addressing the few areas for

improvement, this course can become even more effective in preparing students for the challenges of the engineering profession.

B10502064 王泰傑

This is the course that I will always remember. It reminds me of how unreasonable the world is. The theory always can't explain some actual phenomena. There is always a gap between simulation, prediction, and reality. Working with friends is enjoyable, but not when doing it overnight catching the deadline. Reducing the semester from 18 weeks to 16 weeks makes the whole thing worse. Did I learn anything from the course? Yes, I think. The course greatly demonstrates the current environment of mechanical engineering. Asking the engineers to complete a task with a low budget and want the result to be fairly well in a short period of time. The result will be a group of people working day and night. I don't think the task proposed in this lecture has not validated before, and it's inappropriate to be directly used to evaluate students. The suggestion for the class is that maybe you should add labor costs to the cost limit next year, since the whole thing is not really practical why not make it more realistic?

B10502024 蔡家凱

I want to express my gratitude to my teammates for their outstanding collaboration. Together, we navigated through the challenges of this semester with great synergy, successfully accomplishing our tasks. Throughout our journey, there were hardly any unpleasant moments, which speaks volumes about the positive dynamic within our team. Each member exhibited a commendable sense of responsibility, readily extending support to those facing obstacles along the way.

Being immersed in an environment surrounded by such talented individuals has truly been inspiring. It's in such an atmosphere that one finds the impetus to push their boundaries and strive for excellence. I am genuinely delighted to have had the opportunity to work alongside each of you, as you brought not only your unique strengths but also diverse perspectives to our team, enriching our collective experience.

I believe this course has been immensely beneficial for us, despite the hurdles we encountered, such as the frequent adjustments to the rules and the unpredictable nature of the tests. Beyond the mere evaluation of our test scores, this course has offered us a profound insight into the intricate dynamics of the industry.

In the rapidly evolving realm of technology, foreseeing when development goals—be it client preferences or market conditions—might abruptly shift is virtually impossible. Such shifts can render our prior efforts seemingly futile. The constant adjustments to the rules throughout the course echo the inherent uncertainty that pervades the industry.

While we initially harbored reservations about the rules and pinpointed areas for improvement, our journey through this course has inadvertently equipped us with invaluable experience in adapting swiftly to unforeseen challenges. This adaptability is a critical skill in navigating the ever-changing landscape of technology and underscores the practical relevance of the course material. Through these experiences, we have not only enhanced our understanding of the subject matter but also honed our ability to thrive amidst uncertainty—a skill set indispensable for success in the real-world scenarios we are likely to encounter in our professional endeavors.

## 7. References

- [1] Servo motor MG995 <https://quartzcomponents.com/products/mg995-metal-gear-servo-motor-180-degree-rotation>
- [2] MG90 <https://makersportal.com/shop/mg90s-micro-servo>
- [3] Voltage Converter <https://shop.cpu.com.tw/product/57434/info/>
- [4] TCST2013 <https://www.mouser.tw/ProductDetail/Vishay-Semiconductors/TCST2103?qs=%2Fjqivxn91cc%252BOKE9BUKCsA%3D%3D>
- [5] Elastic Compression of Spheres and Cylinders at Point and Line Contact, Jack A. Stone and Jay H. Zimmerman <https://emtoolbox.nist.gov/Elastic/Case2.asp>
- [6] "Elastic Compression of Spheres and Cylinders at Point and Line Contact," M.J. Puttock and E.G. Thwaite, National Standards Laboratory Technical Paper No. 25, Division of Applied Physics, National Standards Laboratory, Commonwealth Scientific and Industrial Research Organization (CSIRO), University Grounds, Chippendale, New South Wales, Australia 2008, 1969.  
<https://emtoolbox.nist.gov/Publications/NationalStandardsLaboratoryTechnicalPaperNo25.pdf>
- [7] Rod Cross Am. J. Phys. 84, 221–230 (2016). Coulomb's law for rolling friction  
<https://pubs.aip.org/aapt/ajp/article/84/3/221/1057035/Coulomb-s-law-for-rolling-friction>
- [8] Rod Cross 2022 Eur. J. Phys. 43 065002. Measurements of rolling friction with a stringless pendulum <https://iopscience.iop.org/article/10.1088/1361-6404/ac8d3a>

## 8. Appendix

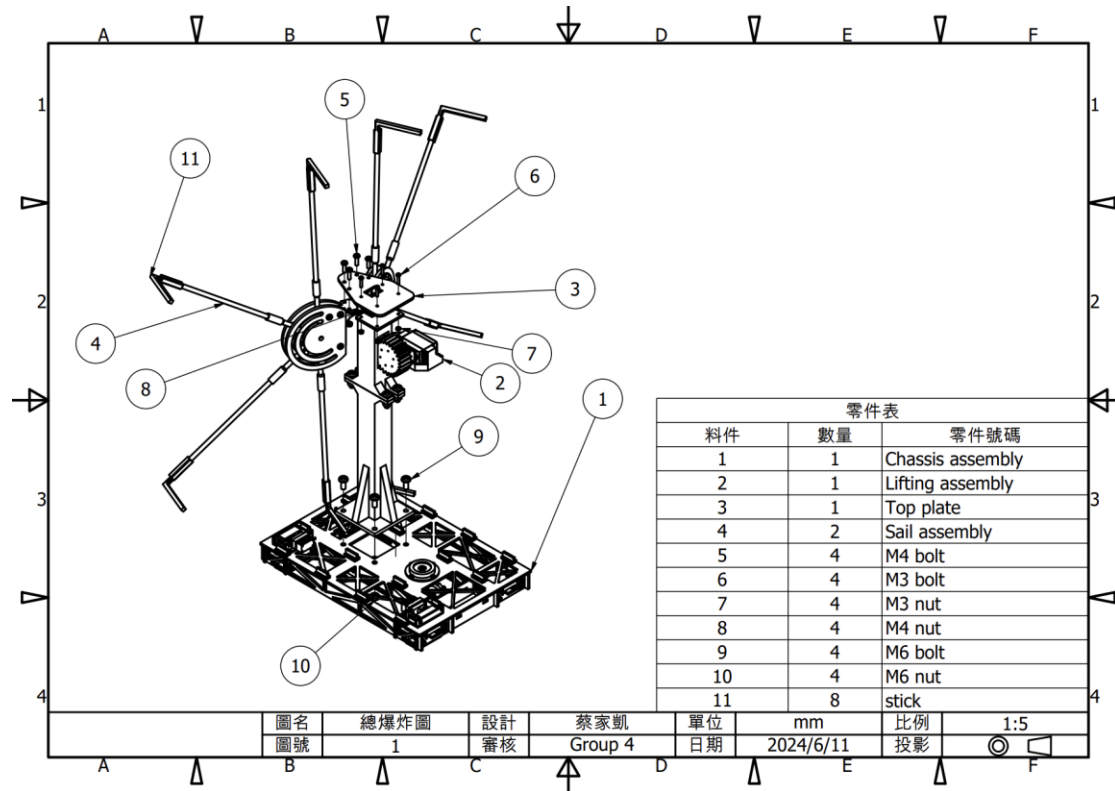
### 8.1 Bill of Materials (BOM)

No.	Part Name	Source	Quantity	Unit Price	Amount
1	Chassis Main Board	Dense Board	1	0	0
2	Chassis Long Frame 1	Dense Board	2	0	0
3	Chassis Long Frame 2	Dense Board	2	0	0
4	Chassis Cross Frame	Dense Board	4	0	0
5	Wheel Frame	Dense Board	4	0	0
6	Pin	Dense Board	24	0	0
7	Bullseye Wheel	Ready-made Part	4	0	0
8	Brake Base	3D Printing	2	0	0
9	Brake Pad	3D Printing	2	0	0
10	Brake Fixing Frame	3D Printing	2	0	0
11	Brake Shim	Dense Board	2	0	0
12	Bearing Holder	3D Printing	1	0	0
13	Bearing	Direct Purchase	1	20	20
14	Holder	3D Printing	1	0	0
15	Encoder Wheel Frame	3D Printing	1	0	0
16	Encoder Tire	Ready-made Part	1	0	0
17	Joint1	3D Printing	1	0	0
18	Joint2	3D Printing	1	0	0
19	Encoder Plate	3D Printing	1	0	0
20	Side1	3D Printing	1	0	0
21	Side2	3D Printing	1	0	0
22	Light-sensitive Board	Direct Purchase	1	40	40
23	Spacer	3D Printing	1	0	0
24	Spring	Ready-made Part	1	0	0
25	M3*25 Rod	3D Printing	1	0	0
26	Front Slide	3D Printing	2	0	0

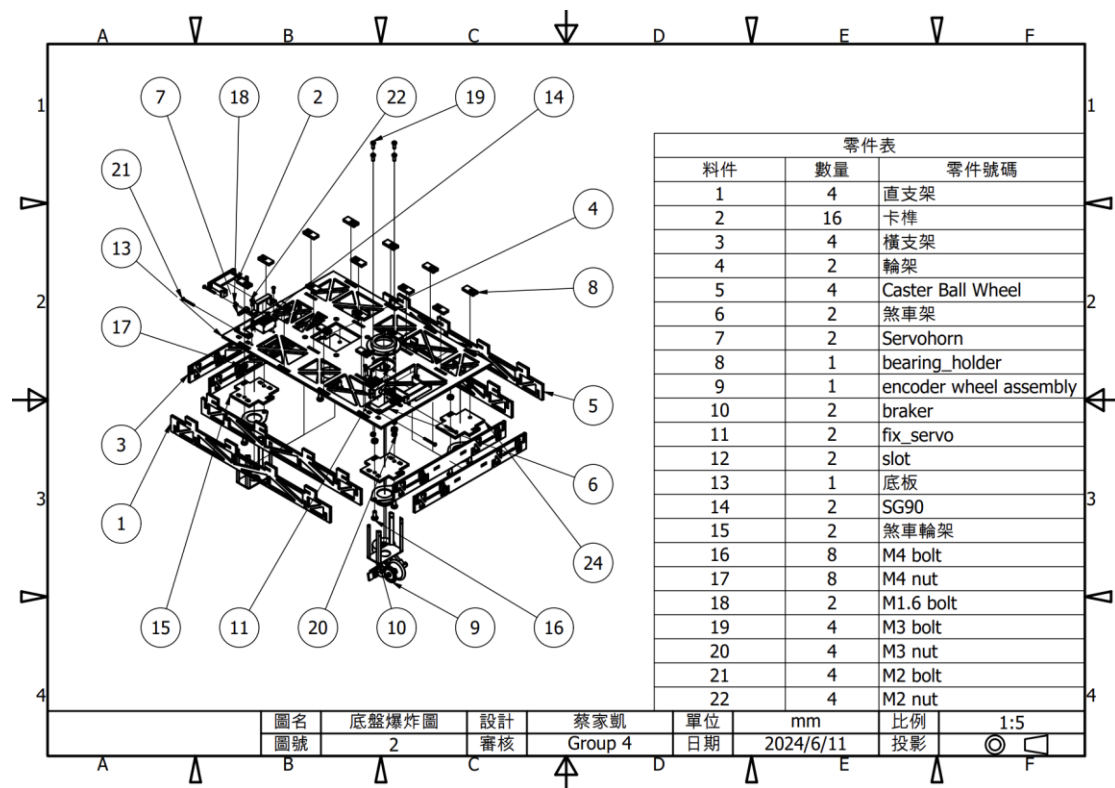
27	Rear Slide	3D Printing	2	0	0
28	Sail Connector	3D Printing	2	0	0
29	Short Slide Pin	3D Printing	4	0	0
30	Long Slide Pin	3D Printing	2	0	0
31	Motor Slide Pin	3D Printing	2	0	0
32	Bamboo Chopsticks for Sail	Ready-made Part	8	0	0
33	Sail	Ready-made Part	2	0	0
34	M2 Screws	Ready-made Part	19	0	0
35	M2 Nuts	Ready-made Part	8	0	0
36	M3 Screws	Ready-made Part	22	0	0
37	M3 Nuts	Ready-made Part	20	0	0
38	M3 Washers	Ready-made Part	6	0	0
39	M4 Screws	Ready-made Part	21	0	0
40	M4 Nuts	Ready-made Part	16	0	0
41	M4 Washers	Ready-made Part	16	0	0
42	MG90	Direct Purchase	4	69	276
43	MG996R	Direct Purchase	1	119	119
44	Single Blade Rudder	Attached Part	2	0	0
45	Cross Rudder	Attached Part	2	0	0
46	Hexagon Rudder	Attached Part	1	0	0
47	Arduino Board	Direct Purchase	1	388	388
48	Breadboard	Direct Purchase	1	50	50
49	Step-down Module	Direct Purchase	1	80	80
50	Battery Holder	Direct Purchase	1	50	50
51	Rechargeable Battery	Direct Purchase	2	99	198
52	Rubber Band	Ready-made Part	3	0	0
53	IMU	Direct Purchase	1	60	60
54	Wires	Direct Purchase	20	7/20	7
55	9V Battery	Direct Purchase	1	41	41
				Total Price	1329

## 8.2 Exploded View

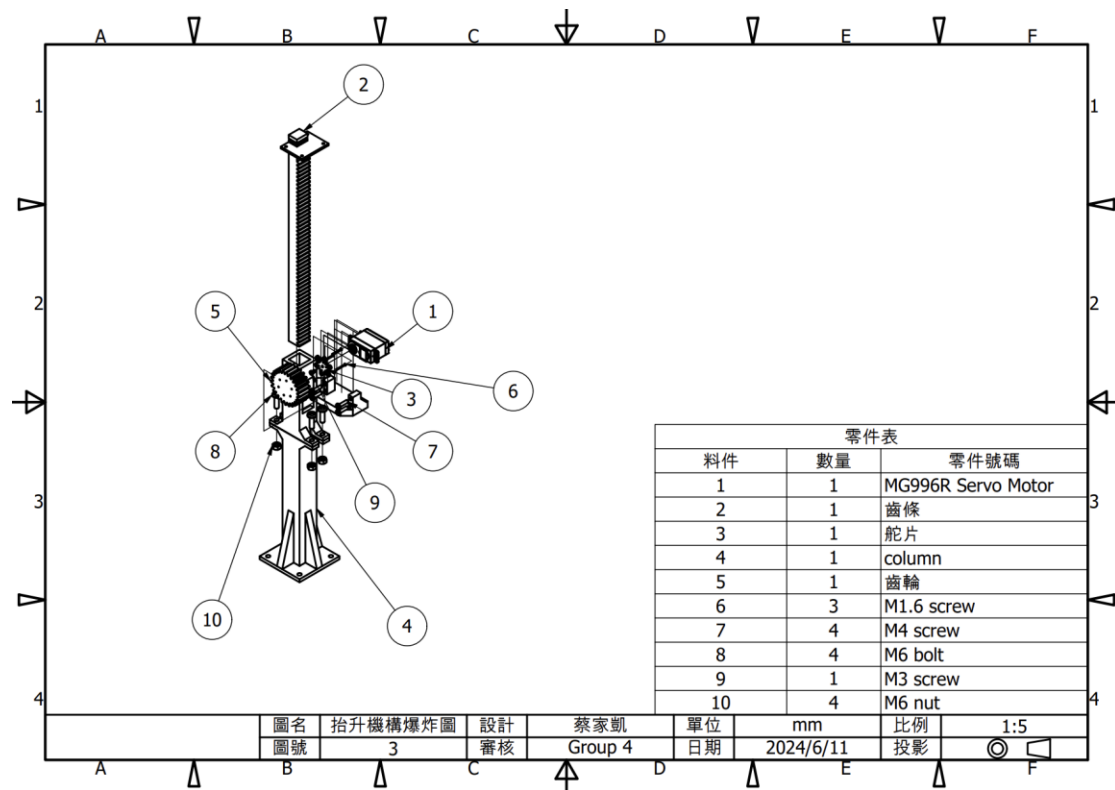
### 8.2.1 Exploded View of the Whole Assembly



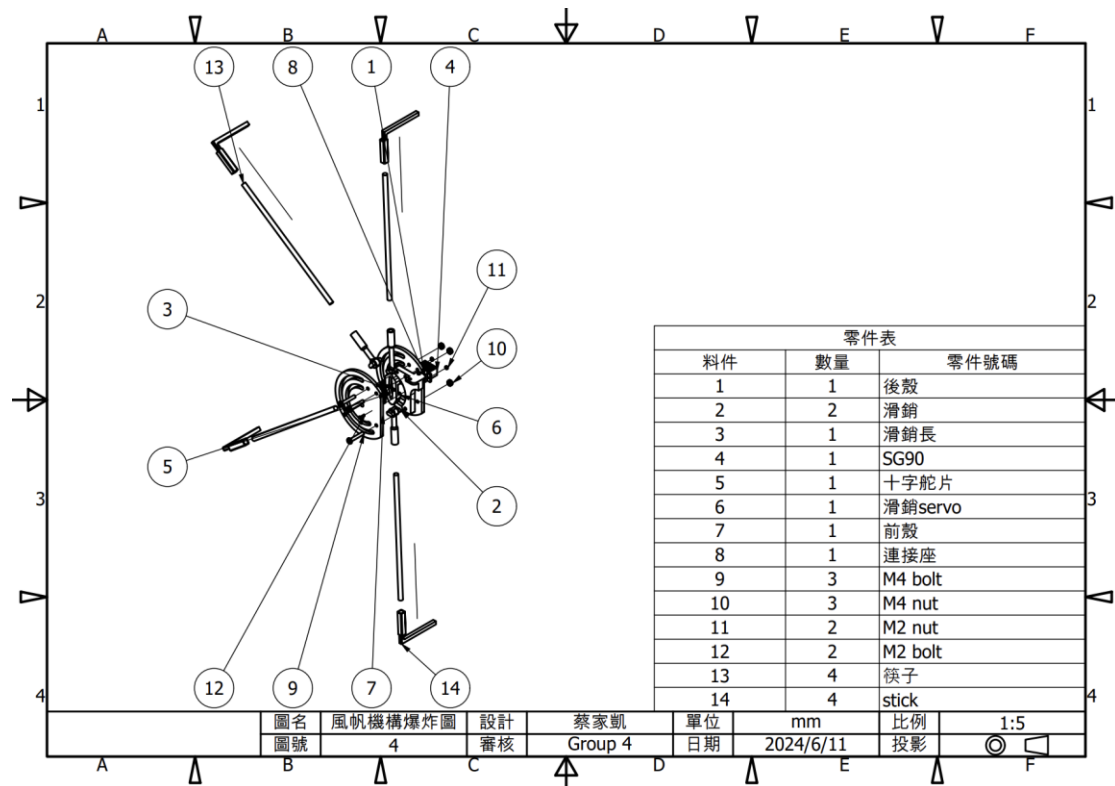
### 8.2.2 Exploded View of the Whole Chassis



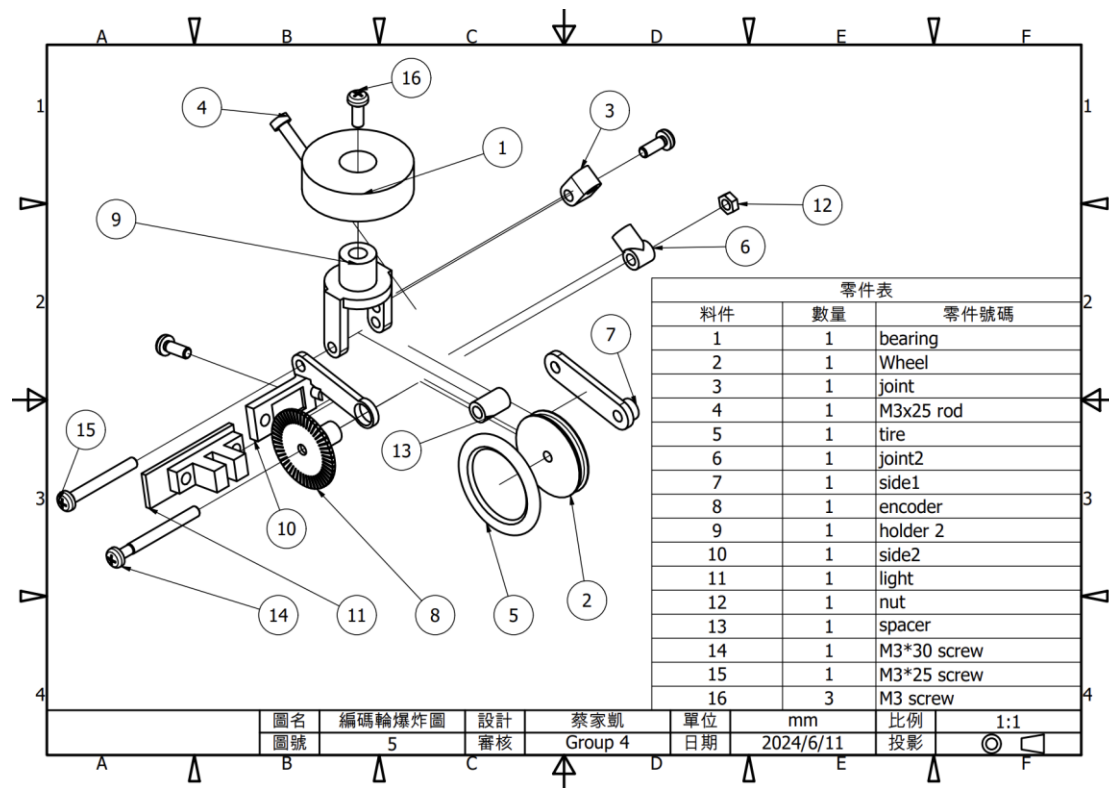
### 8.2.3 Exploded View of the Lifting Mechanism



### 8.2.4 Exploded View of the Sail

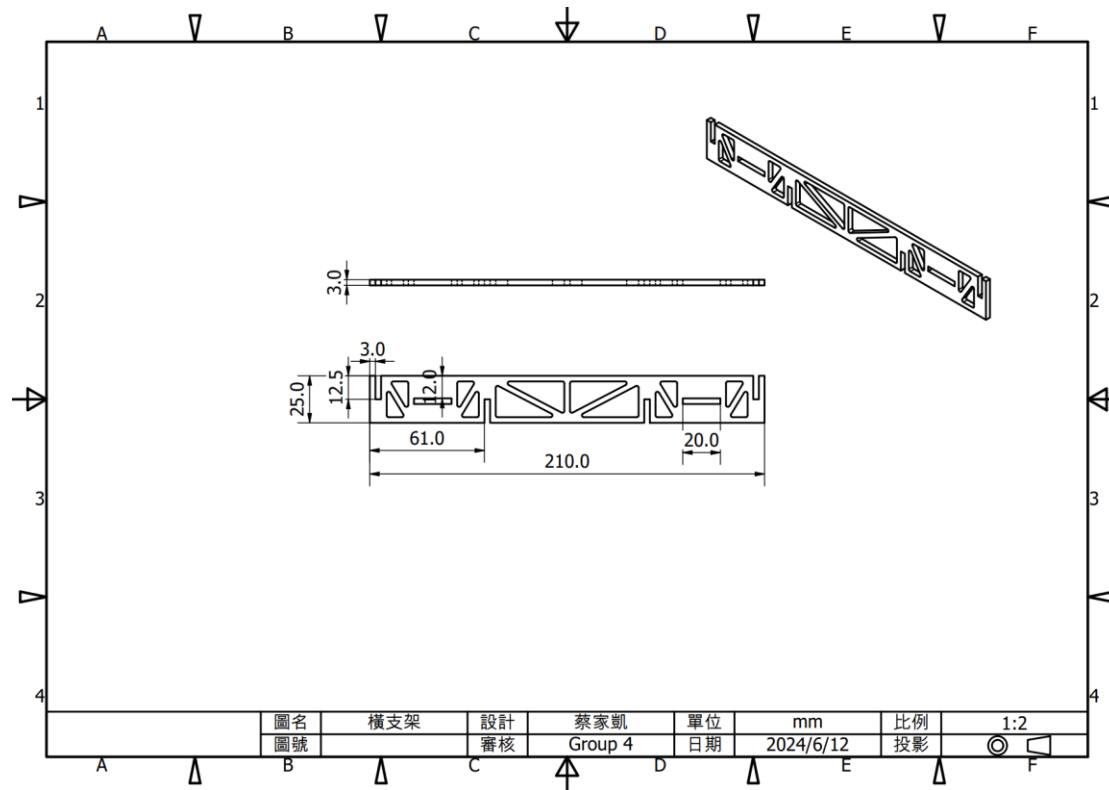


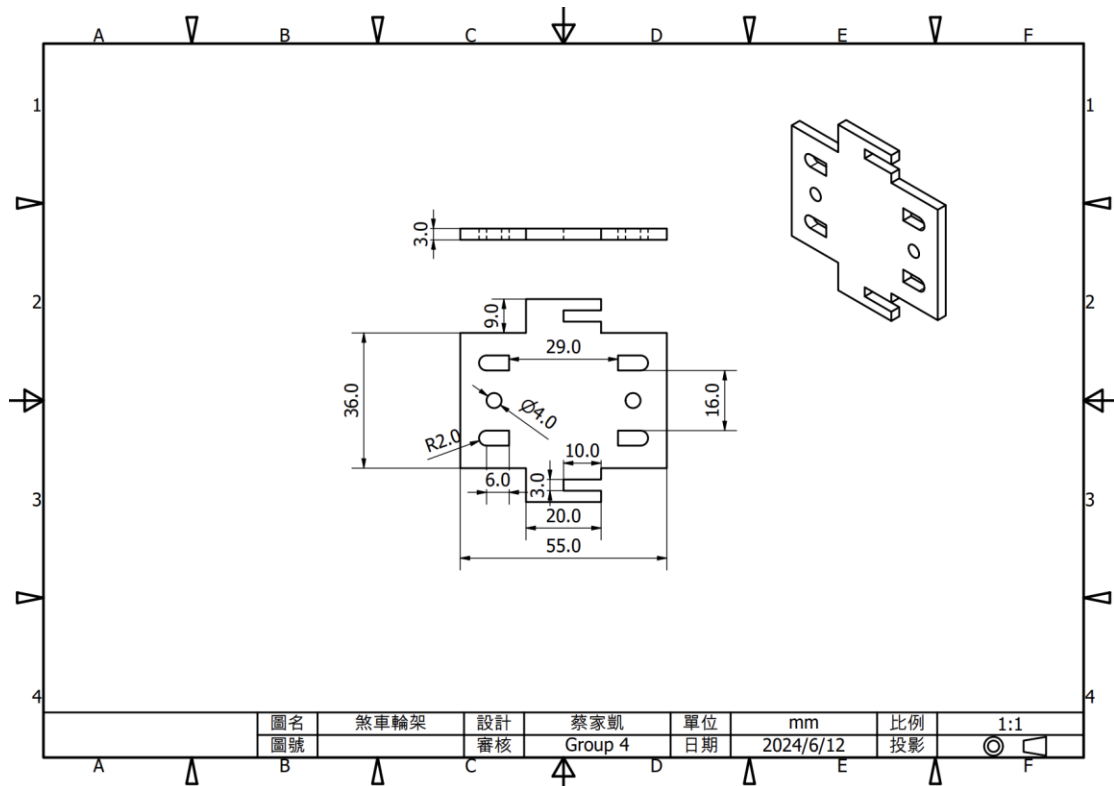
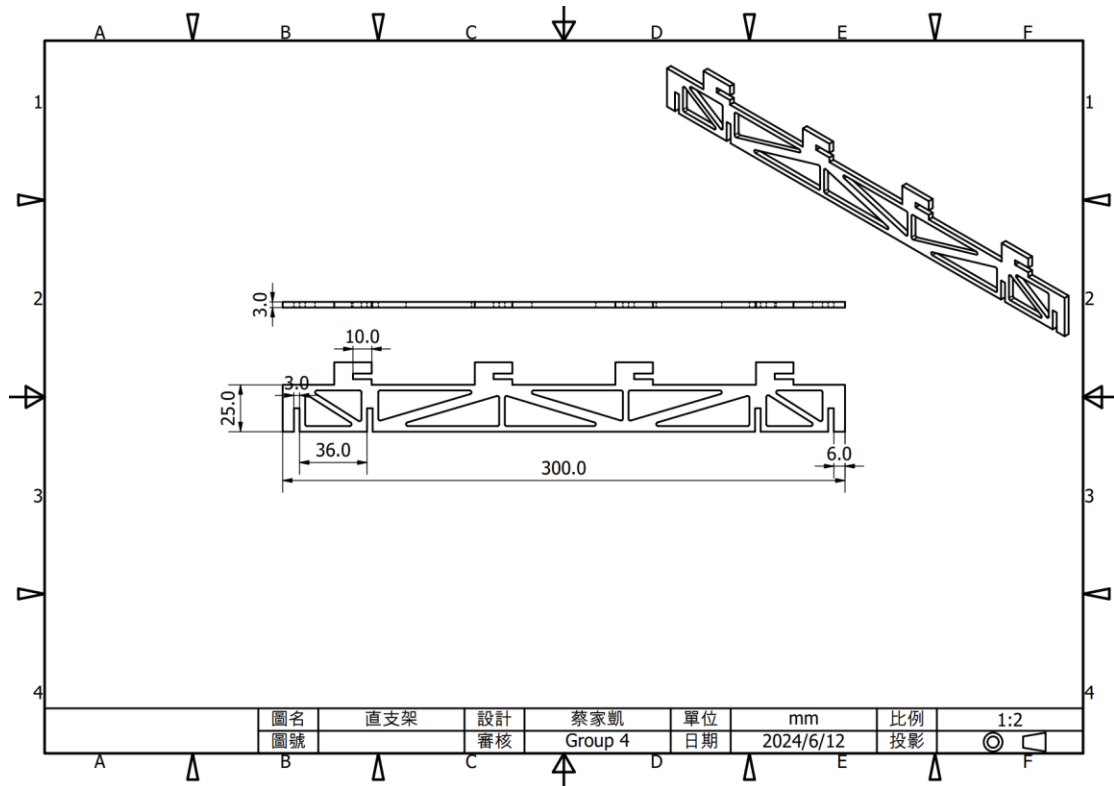
### 8.2.5 Exploded View of the Encoder

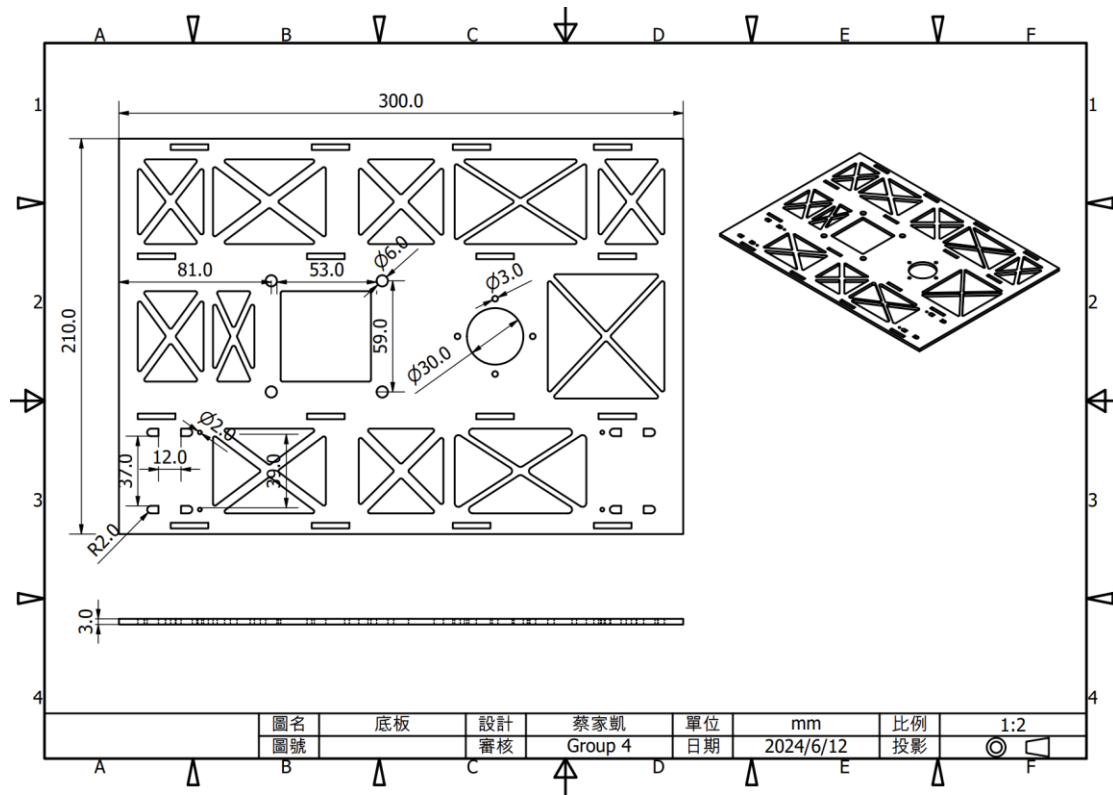


## 8.3 Engineering Drawings of Crucial Components

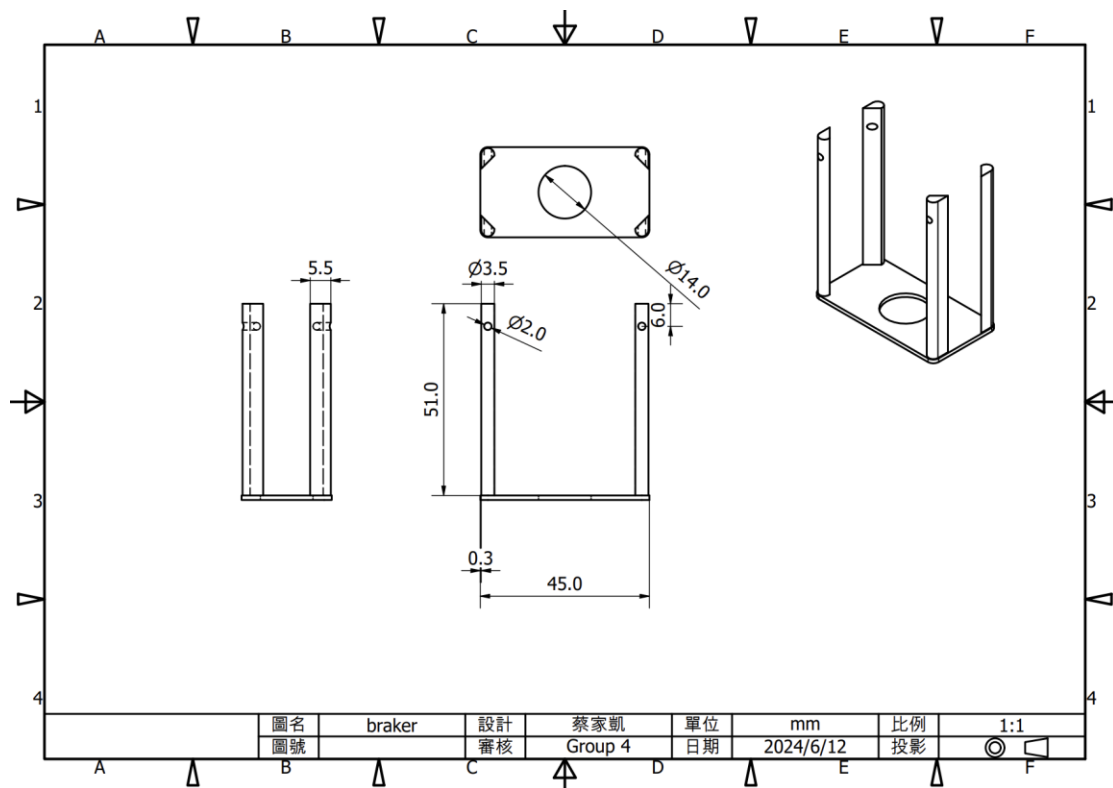
### 8.3.1 Chassis

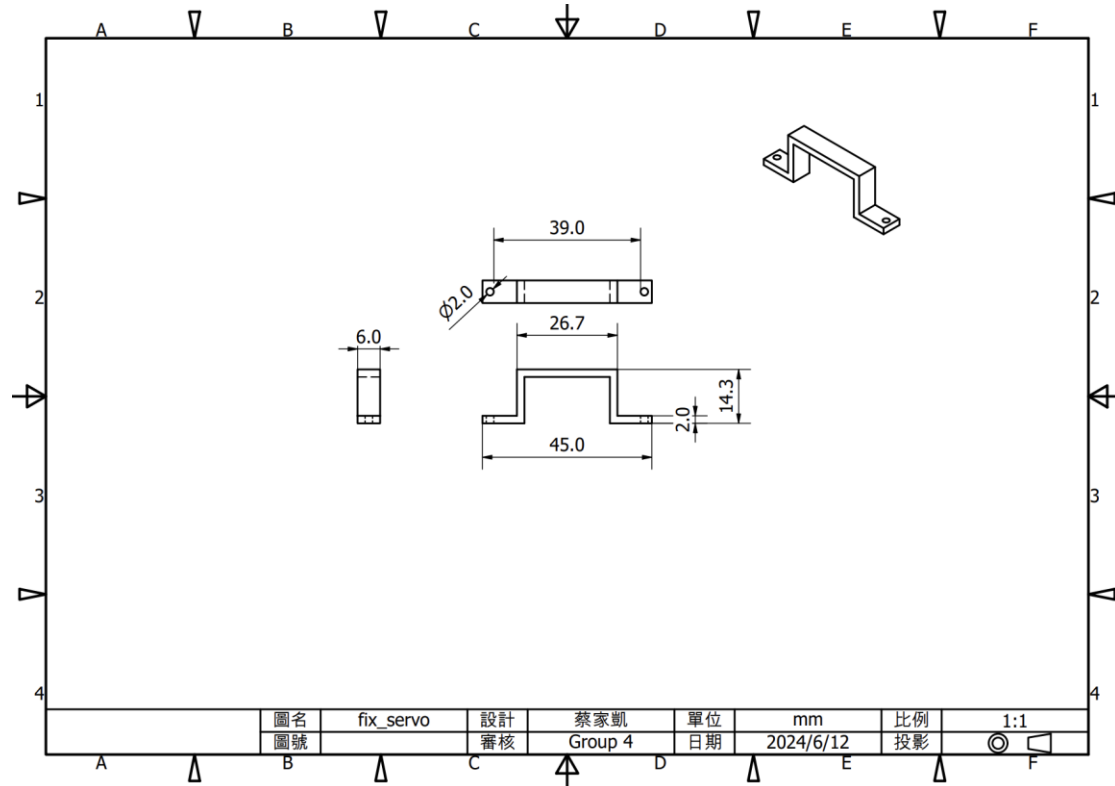
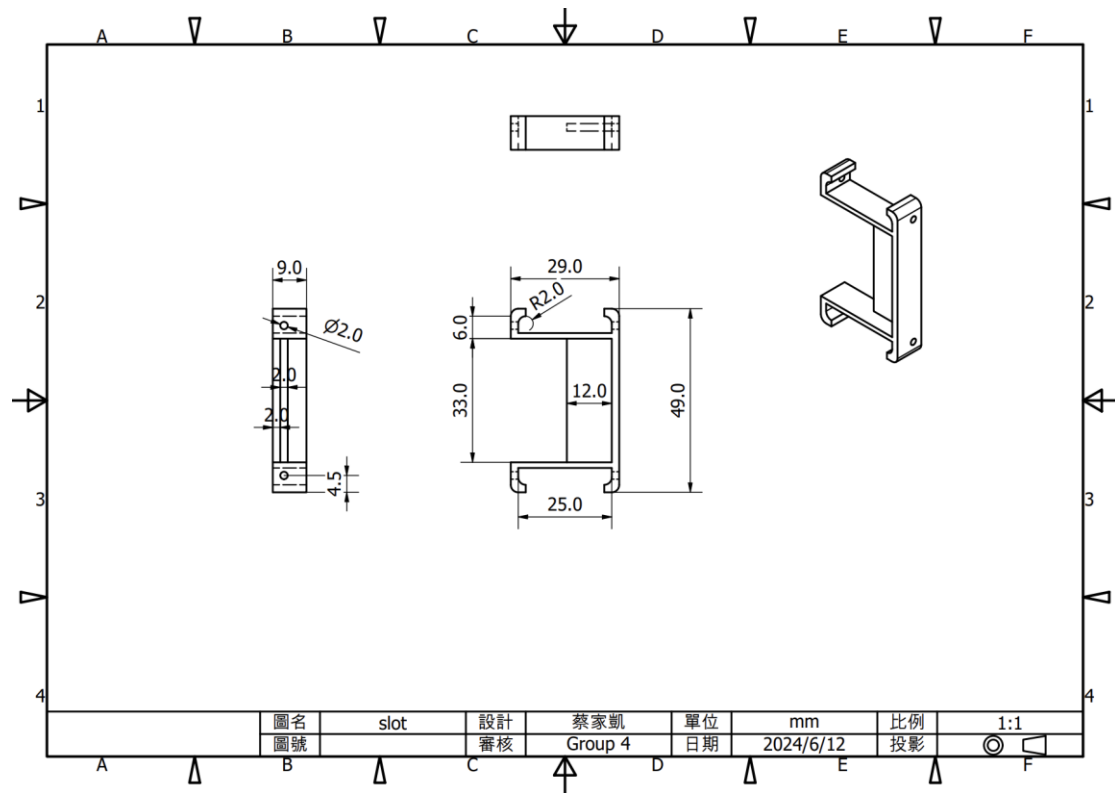




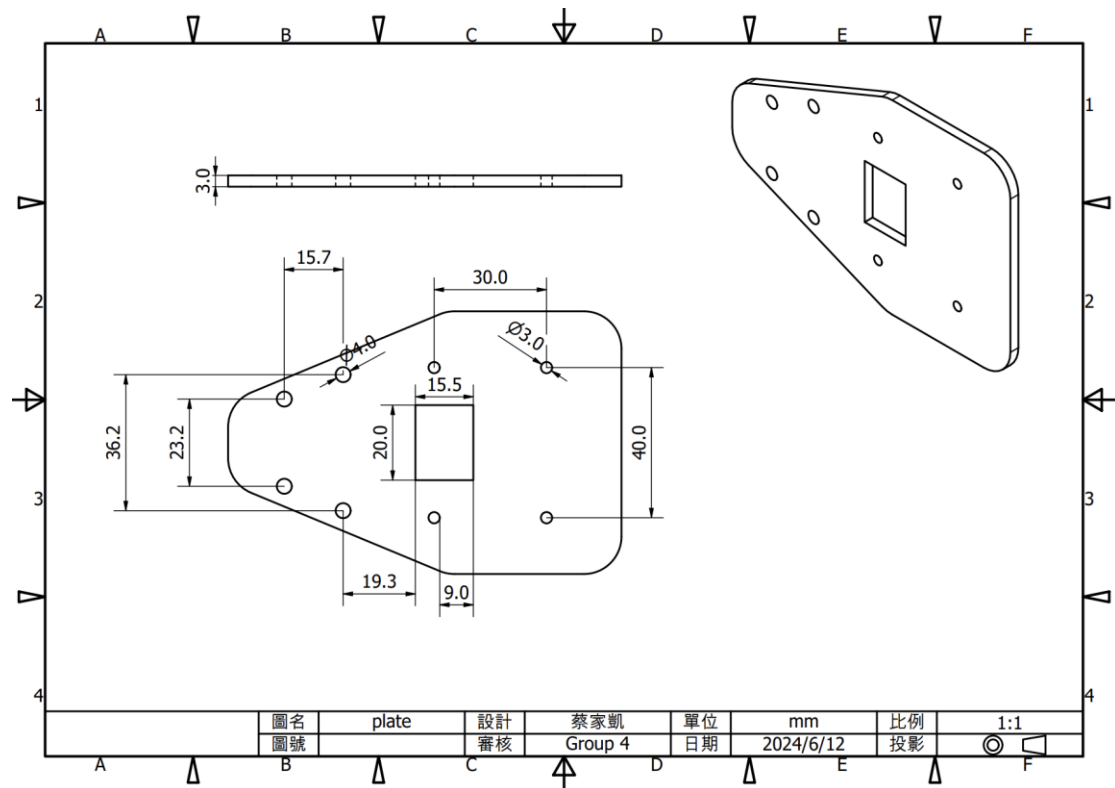
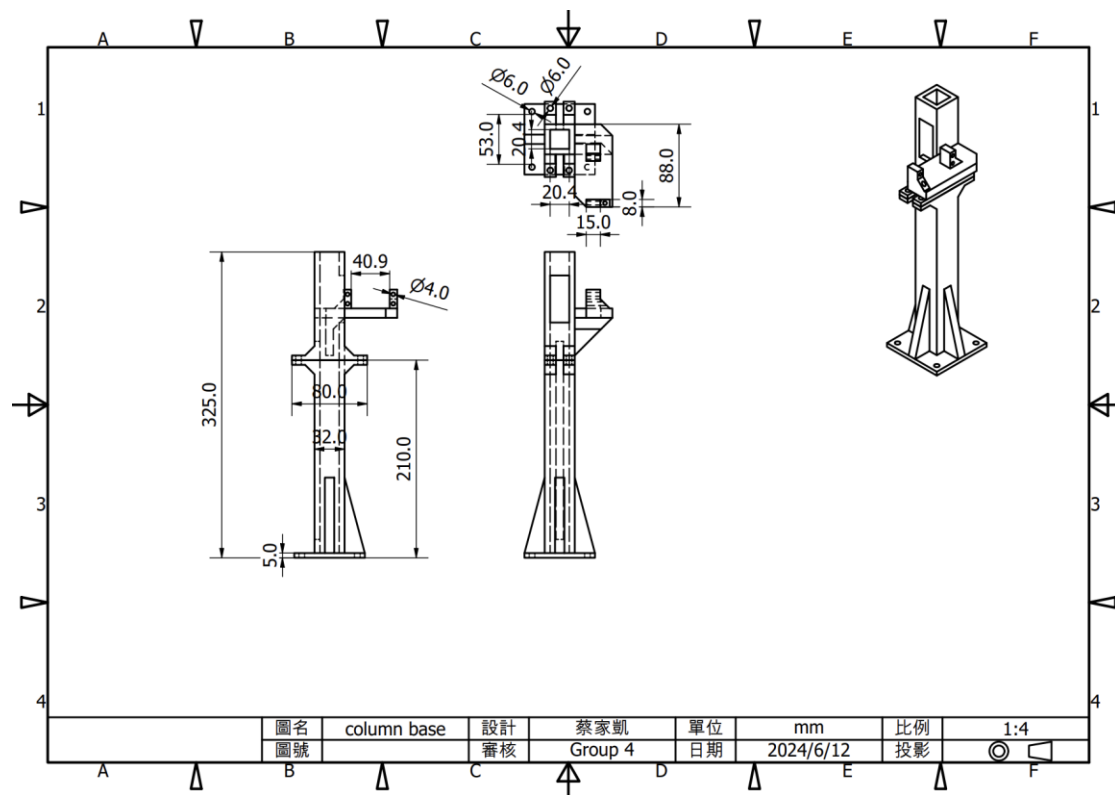


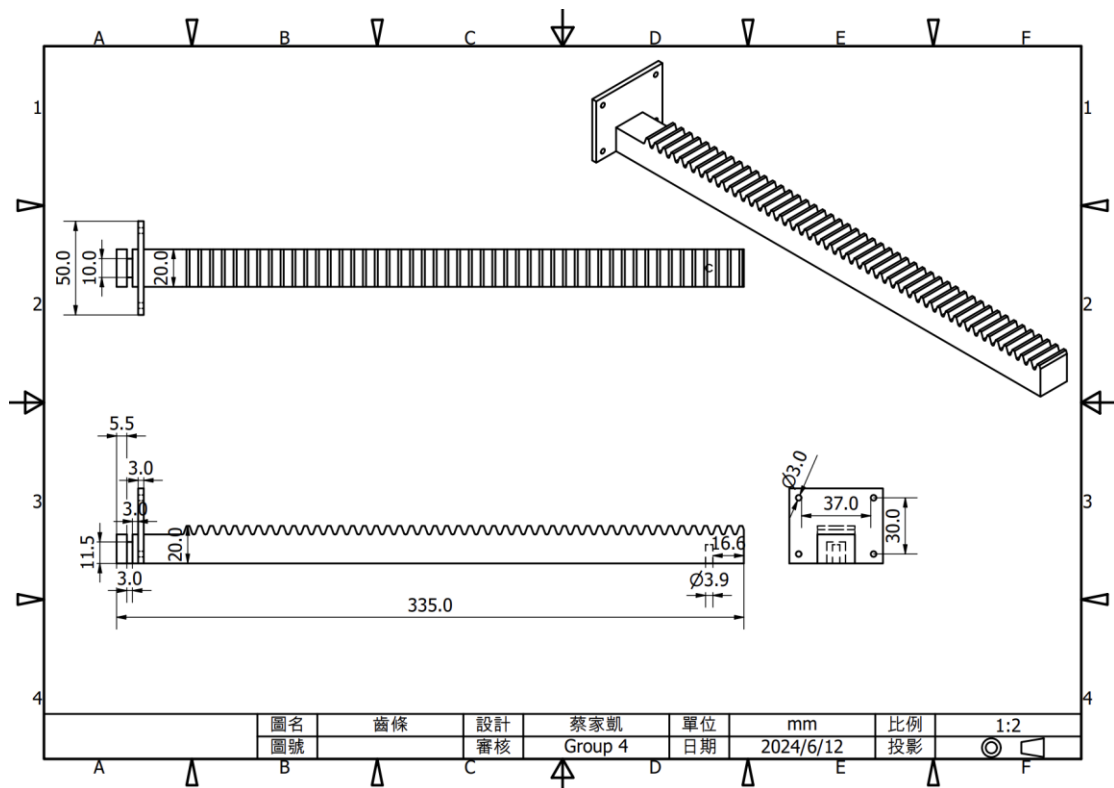
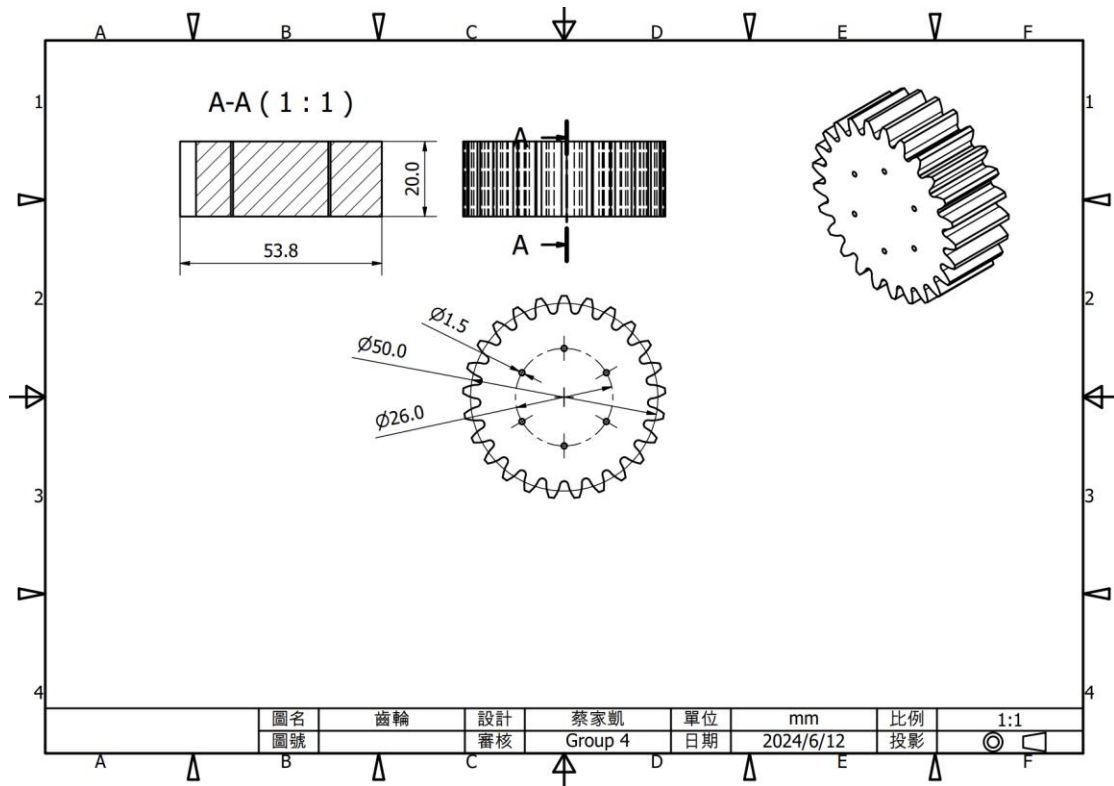
### 8.3.2 Brake



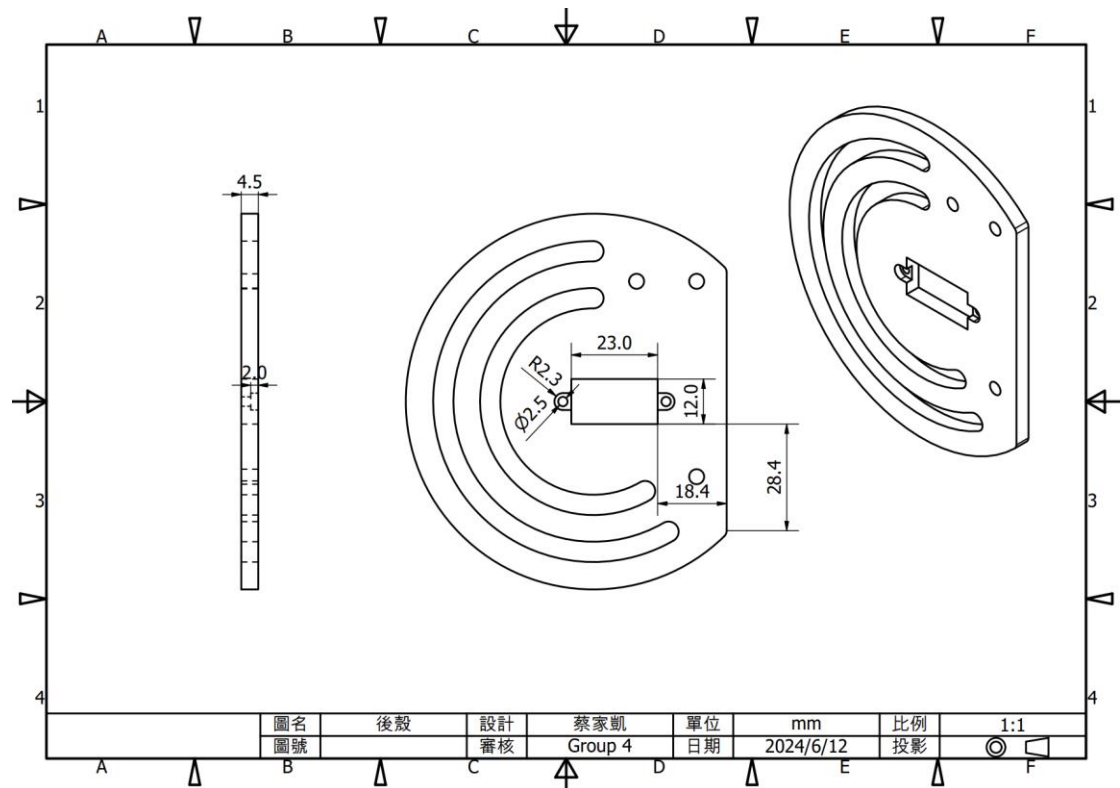
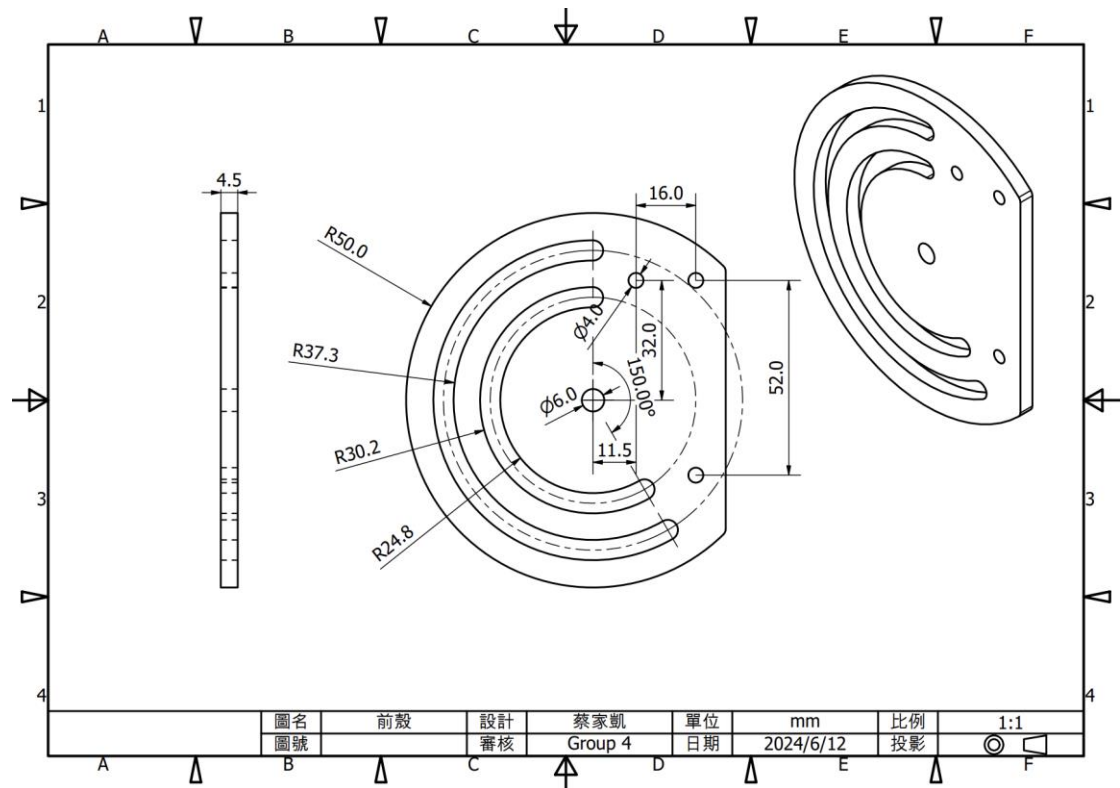


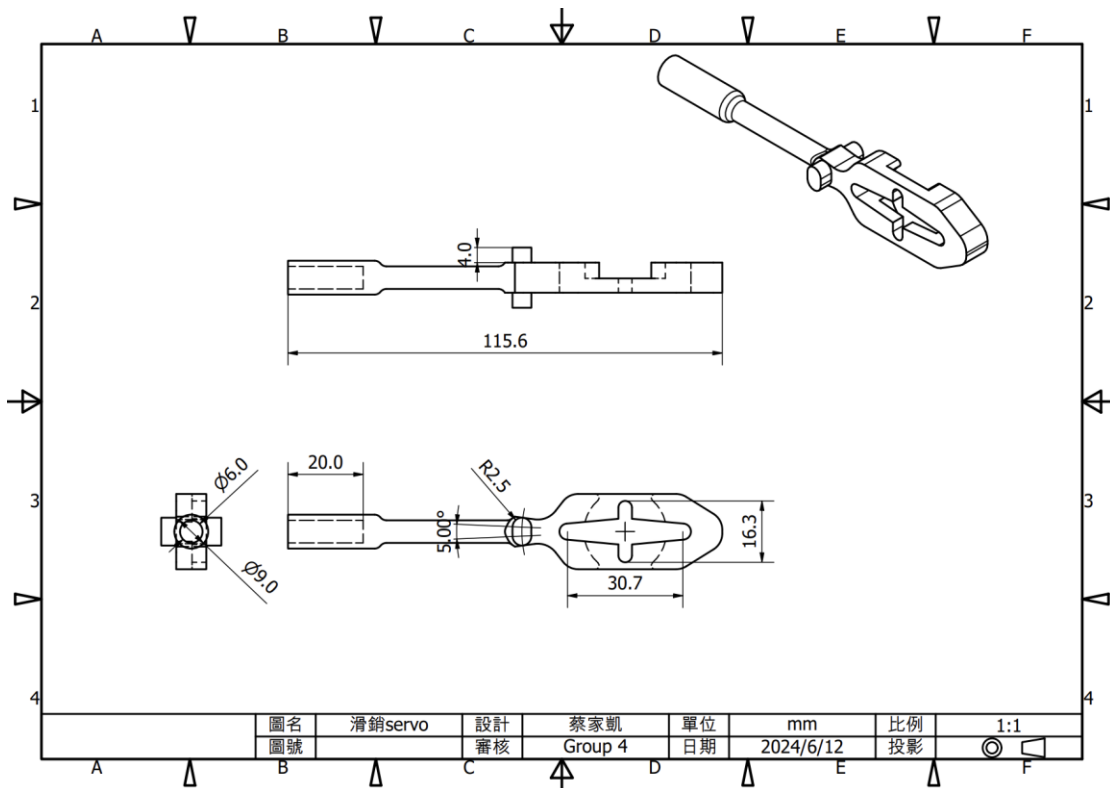
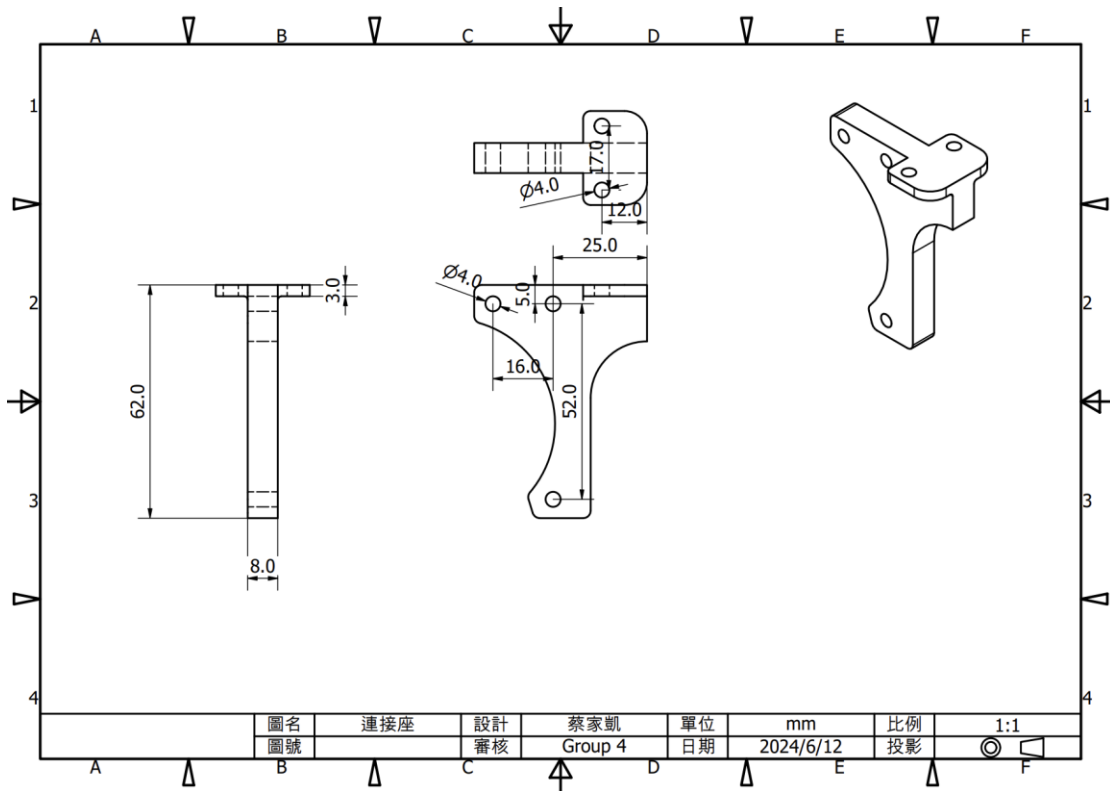
### 8.3.3 Lift

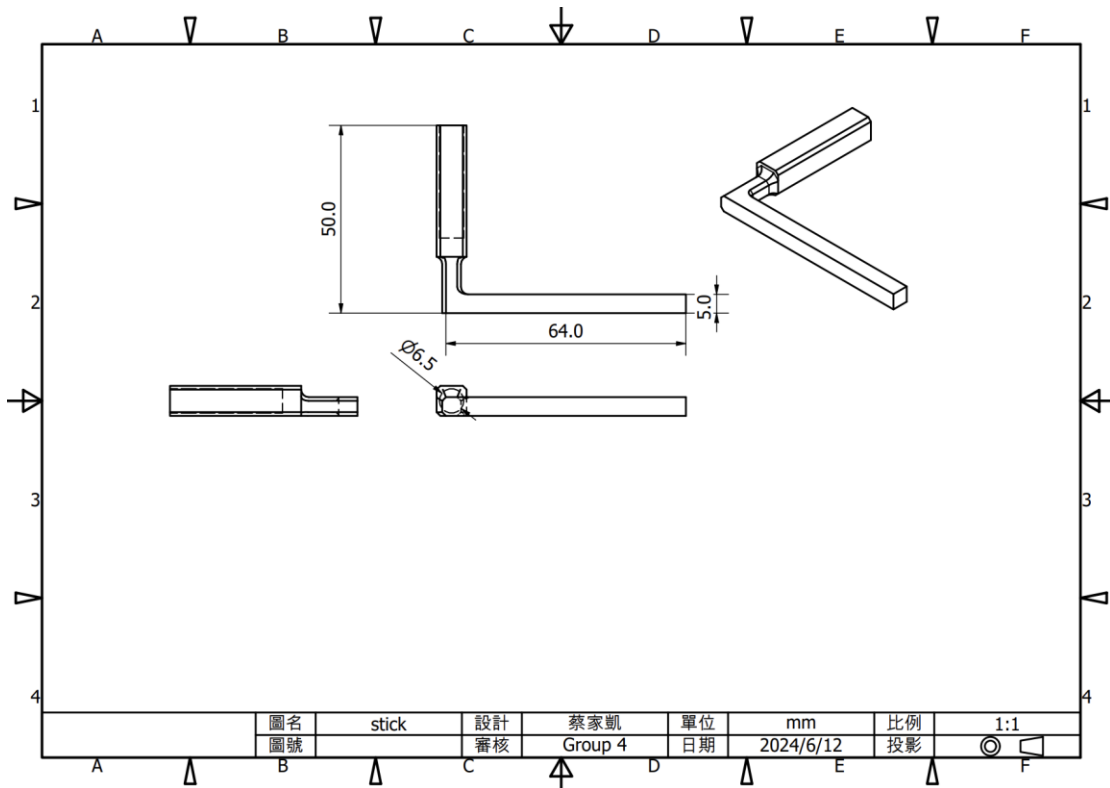
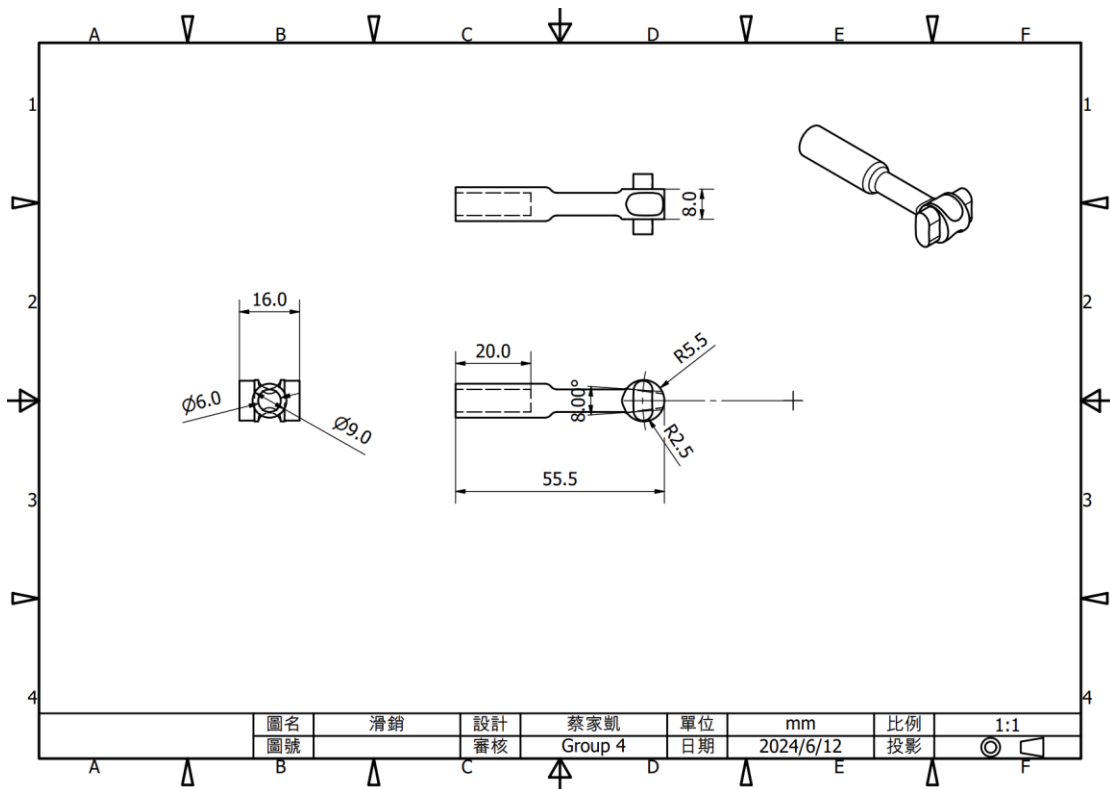




### 8.3.4 Sail







## **8.4 Meeting Minutes**

2/27 Meeting minutes

Topics:

- Team Contract
- Mechanisms needed in the design
- Future Schedule

Conclusions:

- Discuss the team contract next week
  - Everyone has basic ideas about the design and future schedule
  - Discuss the design next week
  - Discuss the schedule after the design is more clear
- 

3/5 Meeting minutes

Topics:

- Team Contract
- Everyone shares their dream car

Conclusions:

- Team contract is set
  - The Gantt chart for the midterm test is set
  - Need more details for the sketch, including the working principle and the advantage of the design
- 

3/10 Meeting minutes

Topics:

- Discuss the sketch
- Chassis design, including 3 or 4 wheels
- Flow field measurement
- Friction of universal wheels

Conclusions:

- The basic subsystems are chassis, lifting mechanism, sail-opening mechanism
  - The friction of each wheel is much different from the others
  - Flywheel may be needed
- 

3/12 Meeting minutes

Topics:

- Sail experiments, including the area, number of sails, angle between the sails, and materials
- Detail of each mechanism

Conclusions:

- Sails prototype

- Chassis design in CAD
  - Lifting mechanism in CAD
  - Flywheel prototype
- 

3/17 Meeting minutes

Topics:

- Sail design
- Chassis design
- Flywheel needed or not

Conclusions:

- Flywheel not needed
  - Sail projection area:  $40 \times 30 \times 2$
  - Start constructing each subsystem
  - Lifting mechanism powered by rubber bands, controlled by SG90
  - Sail-opening mechanism powered by strings, automatically open after lifting
- 

3/24 Meeting minutes

Topics:

- Progress of each subsystem
- Components needed to buy

Conclusions:

- No trouble in any subsystem
  - Continue to construct each subsystem
  - Buy the needed components: Batteries, Arduino UNO, SG90, IMU
- 

3/31 Meeting minutes

Topics:

- Progress of each subsystem
- Work distribution of the midterm analysis report

Conclusions:

- Each subsystem is almost done, assemble all subsystems next week
  - Work distribution is decided
- 

4/7 Meeting minutes

Topics:

- Time for testing and modifying during the week
- The latch for constraining the sail before lifting is needed to be modified

Conclusions:

- Testing and modifying during the week
  - No meeting next week but have to do the analysis report
-

## 4/21 Meeting minutes

Topics:

- Architecture of the new vehicle
- Problems with the midterm vehicle

Conclusions:

- Make the CG (sail) closer to the back of the vehicle
  - Discuss the working principle of the turning control
  - Subsystems unchanged
  - Flow field measurement next week since the runway is still for midterm
- 

## 4/28 Meeting minutes

Topics:

- Prototype for sails
- Working principle of turning control

Conclusions:

- The flow field is weird
  - Sail area control or sail angle control undecided
- 

## 5/2 Meeting minutes

Topics:

- Working principle of turning control

Conclusions:

- Sail area control since easier mechanism
  - Close loop control with position and vehicle heading error feedback
  - Work distribution for each subsystem
  - Add a encoder subsystem
- 

## 5/5 Meeting minutes

Topics:

- Progress of each subsystem
- Components needed to buy

Conclusions:

- No trouble in any subsystem
  - Continue to construct each subsystem
  - Buy the needed components: MG90s for sail opening, MG996 for lifting
- 

## 5/11 Meeting minutes

Topics:

- Progress of each subsystem

- Components needed to buy

Conclusions:

- No trouble in any subsystem
  - Continue to construct each subsystem
- 

5/19 Meeting minutes

Topics:

- Brake system is needed
- Sail-opening mechanism needs help

Conclusions:

- Work distribution for brake and sail-opening mechanism
- 

5/26 Meeting minutes

Topics:

- The vehicle is too heavy to turn enough in the first corner
- Brake system needs help
- Controlling codes for close loop control

Conclusions:

- Make the sails larger
  - Minimize the weight
- 

6/2 Meeting minutes

Topics:

- Arduino UNO interrupt pin (for encoder) is not stable
- MG90s are easily broken
- PD control parameters

Conclusions:

- Buy spare parts
- Test and modify the PD parameters

## 8.5 Code for Testing

```
#include <Servo.h>
#include <Wire.h>

#define PI 3.1415926534
long int Starttime;
bool sailstate = 0;
float Output1;
float Output2;
long int ti;
long int sailtime;
bool sailtimetri = 0;
bool releasestate = 0;

//Encoder
#define encoderPin 3
volatile long int counts = 0;
float distance_mm = 0;

//IMU
const int MPU = 0x68; // MPU6050 I2C address
float AccX, AccY, AccZ;
float GyroX, GyroY, GyroZ;
float accAngleX, accAngleY, gyroAngleX, gyroAngleY, gyroAngleZ;
float roll, pitch, yaw;
float AccErrorX, AccErrorY, GyroErrorX, GyroErrorY, GyroErrorZ;
float elapsedTime, currentTime, previousTime, triggerTime = 100000;
bool trigger = false;
int c = 0;

// Lift
#define motor1Pin 13
#define motor2Pin 12
Servo motor1;
Servo motor2;

// Brake
#define motor3Pin 10
```

```

#define motor4Pin 11
Servo motor3;
Servo motor4;

// Sail
#define motor5Pin 5
#define motor6Pin 6
Servo motor5;
Servo motor6;

// PID
unsigned long lastTime;
double errSum, lastErr;
double kp, ki, kd;
double lastSetpoint = 0, lastError = 0;

//Segment
#define S1 800
#define S2 1100
#define S3 850
#define S4 900

long int tinitial;

void setup() {
    //Encoder
    pinMode(encoderPin, INPUT_PULLUP);
    attachInterrupt(digitalPinToInterrupt(3), doEncoder, FALLING);
    Serial.begin(9600);
    //Servo Motors
    motor1.attach(motor1Pin);
    // motor2.attach(motor2Pin);
    motor3.attach(motor3Pin, 500, 1500);
    motor4.attach(motor4Pin, 500, 1500);
    motor5.attach(motor5Pin);
    motor6.attach(motor6Pin);
    motor3.write(100);
    motor4.write(20);
}

```

```

motor5.write(180);
motor6.write(180);
//IMU
Wire.begin(); // Initialize communication
Wire.beginTransmission(MPU); // Start communication with MPU6050
// MPU=0x68
Wire.write(0x6B); // Talk to the register 6B
Wire.write(0x00); // Make reset - place a 0 into the
6B register
Wire.endTransmission(true);
calculate_IMU_error(); //end the transmission
Starttime = millis();
kp = 15; ki = 0.0;
ti = millis();
kd = 0.4;
tinitial = millis();

}

void loop() {
readIMU();
Serial.println(distance_mm);

if(distance_mm > 600 && !sailstate){ //if sail is not trigger and
distance>1000mm
brake();
rotateLiftingMotors(1800); // lift sail
releasestate = 0;
}
if (distance_mm>=0 && distance_mm <= (S1)){
//Segment 1
if(millis()-ti<400){
brake2();
}
else if(millis()-ti>400&&millis()-ti<600){
brake();
}
}

```

```

else if(millis()-ti>600&&millis()-ti<700){
    releaseBrake();
}
else{
    ti = millis();
}
// if (distance_mm>1500){
//     expandSail();
// }

}

else if (distance_mm>(S1) && distance_mm <= (S1+S2)){

//Segment2

Compute(yaw, 60, 0); //Compute output with input, setpoint ,
midpoint.
motor5.write(Output2);
motor6.write(Output1);

}

else if (distance_mm>(S1+S2) && distance_mm <= (S1+S2+S3)){
//Segment3
Compute(yaw, -30, 60); //Compute output with input, setpoint ,
midpoint.
motor5.write(Output2);
motor6.write(Output1);
}

else if (distance_mm>(S1+S2+S3) && distance_mm <= (S1+S2+S3+S4)){
//Segment4
Compute(yaw, -90, 60); //Compute output with input, setpoint ,
midpoint.
motor5.write(Output2);
if (Output1<=20)
{
    motor6.write(20);
}
}

```

```

    }
    else{
        motor6.write(Output1);
    }
}
else{
    //Segment 5
    Compute(yaw, -90, 0); //Compute output with input, setpoint ,
midpoint.
    motor5.write(Output2);
    motor6.write(20);

}

//Lift
void rotateLiftingMotors(int duration) {
    if (!sailtimetri){
        sailtime = millis(); // Record start time
        sailtimetri = !sailtimetri;
    }
    if (millis() - sailtime < duration) {
        motor1.write(10); // Rotate motor 1 clockwise
        // motor2.write(100); // Rotate motor 2 counterclockwise

    }
    else{
        motor1.write(90);
        sailstate = !sailstate;
    }
    // motor2.write(90);
}

//Brake
void brake() {

```

```

motor3.write(88);
motor4.write(32);
digitalWrite(8,HIGH);
releasestate=0;
}

void releaseBrake()
{
    motor3.write(100);
    motor4.write(20);
    digitalWrite(8,LOW);
}

//Sail
void expandSail()
{
    if(motor5.read()==90)
    {
        return;
    }
    else{
        motor5.write(0);
        motor6.write(0);
    }
}

//Encoder
void doEncoder(){ //encoder 計數的子程式
    counts++;
    distance_mm = (PI*30/50*counts);
}

void calculate_IMU_error() {
    // We can call this function in the setup section to calculate the
    accelerometer and gyro data error. From here we will get the error
    values used in the above equations printed on the Serial Monitor.
}

```

```

// Note that we should place the IMU flat in order to get the proper
values, so that we then can the correct values

// Read accelerometer values 200 times
while (c < 200) {
    Wire.beginTransmission(MPU);
    Wire.write(0x3B);
    Wire.endTransmission(false);
    Wire.requestFrom(MPU, 6, true);
    AccX = (Wire.read() << 8 | Wire.read()) / 16384.0 ;
    AccY = (Wire.read() << 8 | Wire.read()) / 16384.0 ;
    AccZ = (Wire.read() << 8 | Wire.read()) / 16384.0 ;
    // Sum all readings
    AccErrorX = AccErrorX + ((atan((AccY) / sqrt(pow((AccX), 2) +
pow((AccZ), 2))) * 180 / PI));
    AccErrorY = AccErrorY + ((atan(-1 * (AccX) / sqrt(pow((AccY), 2) +
pow((AccZ), 2))) * 180 / PI));
    c++;
}
//Divide the sum by 200 to get the error value
AccErrorX = AccErrorX / 200;
AccErrorY = AccErrorY / 200;
c = 0;
// Read gyro values 200 times
while (c < 200) {
    Wire.beginTransmission(MPU);
    Wire.write(0x43);
    Wire.endTransmission(false);
    Wire.requestFrom(MPU, 6, true);
    GyroX = Wire.read() << 8 | Wire.read();
    GyroY = Wire.read() << 8 | Wire.read();
    GyroZ = Wire.read() << 8 | Wire.read();
    // Sum all readings
    GyroErrorX = GyroErrorX + (GyroX / 131.0);
    GyroErrorY = GyroErrorY + (GyroY / 131.0);
    GyroErrorZ = GyroErrorZ + (GyroZ / 131.0);
    c++;
}
//Divide the sum by 200 to get the error value

```

```

GyroErrorX = GyroErrorX / 200;
GyroErrorY = GyroErrorY / 200;
GyroErrorZ = GyroErrorZ / 200;
// Print the error values on the Serial Monitor
Serial.print("AccErrorX: ");
Serial.println(AccErrorX);
Serial.print("AccErrorY: ");
Serial.println(AccErrorY);
Serial.print("GyroErrorX: ");
Serial.println(GyroErrorX);
Serial.print("GyroErrorY: ");
Serial.println(GyroErrorY);
Serial.print("GyroErrorZ: ");
Serial.println(GyroErrorZ);
}

void readIMU(){
// === Read accelerometer data ===
Wire.beginTransmission(MPU);
Wire.write(0x3B); // Start with register 0x3B (ACCEL_XOUT_H)
Wire.endTransmission(false);
Wire.requestFrom(MPU, 6, true); // Read 6 registers total, each axis
value is stored in 2 registers
//For a range of +-2g, we need to divide the raw values by 16384,
according to the datasheet
AccX = (Wire.read() << 8 | Wire.read()) / 16384.0; // X-axis value
AccY = (Wire.read() << 8 | Wire.read()) / 16384.0; // Y-axis value
AccZ = (Wire.read() << 8 | Wire.read()) / 16384.0; // Z-axis value
// Calculating Roll and Pitch from the accelerometer data
accAngleX = (atan(AccY / sqrt(pow(AccX, 2) + pow(AccZ, 2))) * 180 /
PI) - 0.58; // AccErrorX ~(-0.58) See the calculate_IMU_error() custom
function for more details
accAngleY = (atan(-1 * AccX / sqrt(pow(AccY, 2) + pow(AccZ, 2))) * 180
/ PI) + 1.58; // AccErrorY ~(1.58)
// === Read gyroscope data ===
previousTime = currentTime; // Previous time is stored before
the actual time read
currentTime = millis(); // Current time actual time read
}

```

```

elapsedTime = (currentTime - previousTime) / 1000; // Divide by 1000
to get seconds

Wire.beginTransmission(MPU);
Wire.write(0x43); // Gyro data first register address 0x43
Wire.endTransmission(false);
Wire.requestFrom(MPU, 6, true); // Read 4 registers total, each axis
value is stored in 2 registers
GyroX = (Wire.read() << 8 | Wire.read()) / 131.0; // For a 250deg/s
range we have to divide first the raw value by 131.0, according to the
datasheet
GyroY = (Wire.read() << 8 | Wire.read()) / 131.0;
GyroZ = (Wire.read() << 8 | Wire.read()) / 131.0;
// Correct the outputs with the calculated error values
GyroX = GyroX - GyroErrorX; // GyroErrorX ~(-0.56)
GyroY = GyroY - GyroErrorY; // GyroErrorY ~(2)
GyroZ = GyroZ - GyroErrorZ; // GyroErrorZ ~ (-0.8)
// Currently the raw values are in degrees per seconds, deg/s, so we
need to multiply by sendonds (s) to get the angle in degrees
gyroAngleX = gyroAngleX + GyroX * elapsedTime; // deg/s * s = deg
gyroAngleY = gyroAngleY + GyroY * elapsedTime;
yaw = yaw + GyroZ * elapsedTime;
// Complementary filter - combine acceleromter and gyro angle values
roll = 0.96 * gyroAngleX + 0.04 * accAngleX;
pitch = 0.96 * gyroAngleY + 0.04 * accAngleY;

// Serial.println("In IMU");
}

void Compute(double Input, double Setpoint, double midpoint){
unsigned long now = millis();
double timeChange = (double)(now-lastTime);
double error = Setpoint-Input;
errSum += (error*timeChange);
double dErr = (error-lastErr)/ timeChange;
double delta = kp*error + ki*errSum + kd*dErr;
Output1 = midpoint + delta;
Output2 = midpoint - delta;
if(Output1 >150){

```

```
    Output1 = 150;
}
if(Output1 <0){
    Output1 = 0;
}
if(Output2 >150){
    Output2 = 150;
}
if(Output2 <0){
    Output2 = 0;
}
lastError = error;
lastTime = now;

}
```